Palaeogeography, Palaeoclimatology, Palaeoecology 510 (2018) 63–77

Contents lists available at ScienceDirect

Palaeogeography, Palaeoclimatology, Palaeoecology

journal homepage: www.elsevier.com/locate/palaeo

Quantitative reconstruction of Middle and Late Eocene paleoclimate based on palynological records from the Huadian Basin, northeastern China: Evidence for monsoonal influence on oil shale formation

Qing-tao Meng[a,b,c,*], Angela A. Bruch[d], Ge Sun[b,e], Zhao-jun Liu[a,b,c], Fei Hu[a,b,c], Ping-chang Sun[a,b,c]

[a] College of Earth Sciences, Jilin University, Changchun, Jilin 130061, China
[b] Key-Lab for Evolution of Past Life and Environment in Northeast Asia, Ministry of Education, Changchun, Jilin 130026, China
[c] Key-Lab for Oil Shale and Paragenetic Minerals of Jilin Province, Changchun, Jilin 130061, China
[d] Senckenberg Research Institute and Natural History Museum, Frankfurt 60325, Germany
[e] College of paleontology, Shenyang Normal University, Shenyang, Liaoning 110034, China

ARTICLE INFO

Keywords:
Eocene cooling
Seasonality
Quantitative climate reconstruction
East Asian Monsoon
Nearest living relatives
Palynology

ABSTRACT

The Eocene was an interval of climate evolution, when the extreme high temperatures of the earliest Cenozoic gave way to a global cooling trend. Fine-grained lacustrine sediments of Eocene age from northeastern China represent an excellent archive to study long-term environmental and climatic changes at high-resolution. The Huadian Basin is a Cenozoic, fault-bounded basin in Jilin Province, northeastern China. Though small in area, it contains numerous oil shale- and coal-bearing layers, which provide an abundant Middle to Late Eocene palynoflora. Eighty-five palynomorph genera and one hundred palynomorph species were identified in the Huadian Formation, allowing to distinguish 4 palynozones. The nearest living relatives of the recovered palynomorph taxa suggest the presence of subtropical evergreen and deciduous broad-leaved forests during deposition of the Huadian Formation.

Using the coexistence approach (CA), we calculated seven paleoclimatic parameters, which indicate a subtropical warm and humid climate with a mean annual temperature above 13.6 °C and a mean annual precipitation of at least 887 mm. However, the climate became cooler and drier during the transition from the lower Oil Shale Member to the upper Carbonaceous Shale Member. Palaeoclimatic data from the various Middle and Late Eocene basins of northeastern China (i.e., the Huadian, Fushun, Yilan, Hunchun and Jishu basins) were compared with data from North American and European basins. Middle Eocene climate in the Northern Hemisphere was generally warm and humid, and the mean annual temperature and precipitation in northeastern China were similar to those in North America, though slightly lower than those of Europe. Similar trends in temperature and precipitation on different continents support the existence of a global Mid-Eocene cooling event.

This paper is the first systematic study of Middle to Late Eocene seasonality in the Huadian Basin. Our results show an apparent differentiation in both temperature and precipitation between summer and winter, supporting the view that the East Asian Monsoon was established in northeastern China already during the Middle to Late Eocene. This Middle and Late Eocene monsoon was likely driven by the development of Pacific trade winds and an alternating, seasonal high- and low-pressure system over Siberia.

The climatic changes observed in our dataset, especially the precipitation changes, appear to have played an important role in controlling oil shale formation in the Huadian Basin. A warmer and more humid climate, with abundant precipitation and high subsidence rates, formed a deeper Huadian depositional lake. High productivity and stable stratification provided the abundant organic matter and favorable preservation conditions necessary for oil shale accumulation.

* Corresponding author at: College of Earth Sciences, Jilin University, Changchun 130061, China.
E-mail address: mengqt@jlu.edu.cn (Q.-t. Meng).

https://doi.org/10.1016/j.palaeo.2017.11.036
Received 4 May 2017; Received in revised form 14 November 2017; Accepted 14 November 2017
Available online 16 November 2017
0031-0182/ © 2017 Elsevier B.V. All rights reserved.

1. Introduction

As global climatic and environmental changes become increasingly prominent, the history of regional and global climatic evolution has received growing attention. Geological records offer direct evidence of past environmental change, and allow for the quantitative reconstruction of past climatic systems, which will be vital when estimating the consequences of future climate change (Utescher and Mosbrugger, 2007; Zachos et al., 2008; Grein et al., 2011). The Eocene represents a crucial period of Cenozoic climatic evolution, when the global climate transitioned from an extremely warm, ice-free "greenhouse" world in the latest Paleocene-earliest Eocene (P/E) to a cool "icehouse" world by the Eocene-Oligocene transition (E/O) (Zachos et al., 1994, 2001, 2008; Greenwood and Wing, 1995; Wilf, 2000; Irving, 2008; Eldrett and Harding, 2009; Wang et al., 2009; Su et al., 2009). The Eocene evolution of global climate has been extensively studied, using fossil plant assemblages from Australia, Europe, and North America (Wing and Greenwood, 1993, Wing et al., 1999; Greenwood and Wing, 1995; Wilf et al., 1998, Wilf, 2000; Greenwood et al., 2010; Mosbrugger et al., 2005), as well as marine data from both hemispheres (Zachos et al., 2001; Tripati et al., 2005; Villa et al., 2008; Hollis et al., 2009; Passchier et al., 2009; Grein et al., 2011). However, there are few reconstructions of Eocene climate based on terrestrial data from East Asia (He and Tao, 1997; Su et al., 2009; Wang et al., 2010; Meng et al., 2012a, b; Quan et al., 2012), a region with important implications for understanding the Eocene climatic system.

Northeastern China (Fig. 1A) is located at the eastern margin of the Eurasian continent, close to Siberia and the Pacific Ocean. Thus, it is sensitive to climatic changes, and records early and strong signals of global change (Wang, 1998). Eocene strata are widely distributed in northeastern China in a number of small fault-controlled basins, which are concentrated in the Dunhua-Mishan and Yilan-Yitong fault zones, the two northern branches of the Tanlu Fault (Fig. 1B). These basins contained lakes that persisted over long periods of time, allowing thick successions of organic-rich sediments to accumulate under reducing conditions. As a result, these basins now contain abundant oil, gas, oil shale, and coal resources. Oil shales and coals are some of the finest-grained sediments deposited in continental environments, and are sensitive, high-resolution natural archives of paleoclimatic and paleoenvironmental information (Kelts and Hsü, 1978; Wei and Wan, 1995; Wang and Mei, 1998; Zhu et al., 2005; Liu et al., 2009, 2012; Meng et al., 2012a, b, Meng et al., 2013).

The Huadian Basin (42.9°–43° N, 126.7°–126.9° E) is located in the Huadian area of Jilin Province, northeastern China. It has an area of 40 km^2 and is well-known as an oil shale- and coal-bearing basin. The Eocene Huadian Formation has a maximum thickness of > 1000 m. These thick lacustrine deposits provide an exceptional high-resolution record of environmental and climatic change over a long time span.

So far, there has been no detailed study of the Eocene palynoflora in Huadian Basin and its climatic implications. This paper aims to systematically assess the characteristics of lacustrine palynomorph assemblages, and to quantitatively reconstruct climatic changes in the

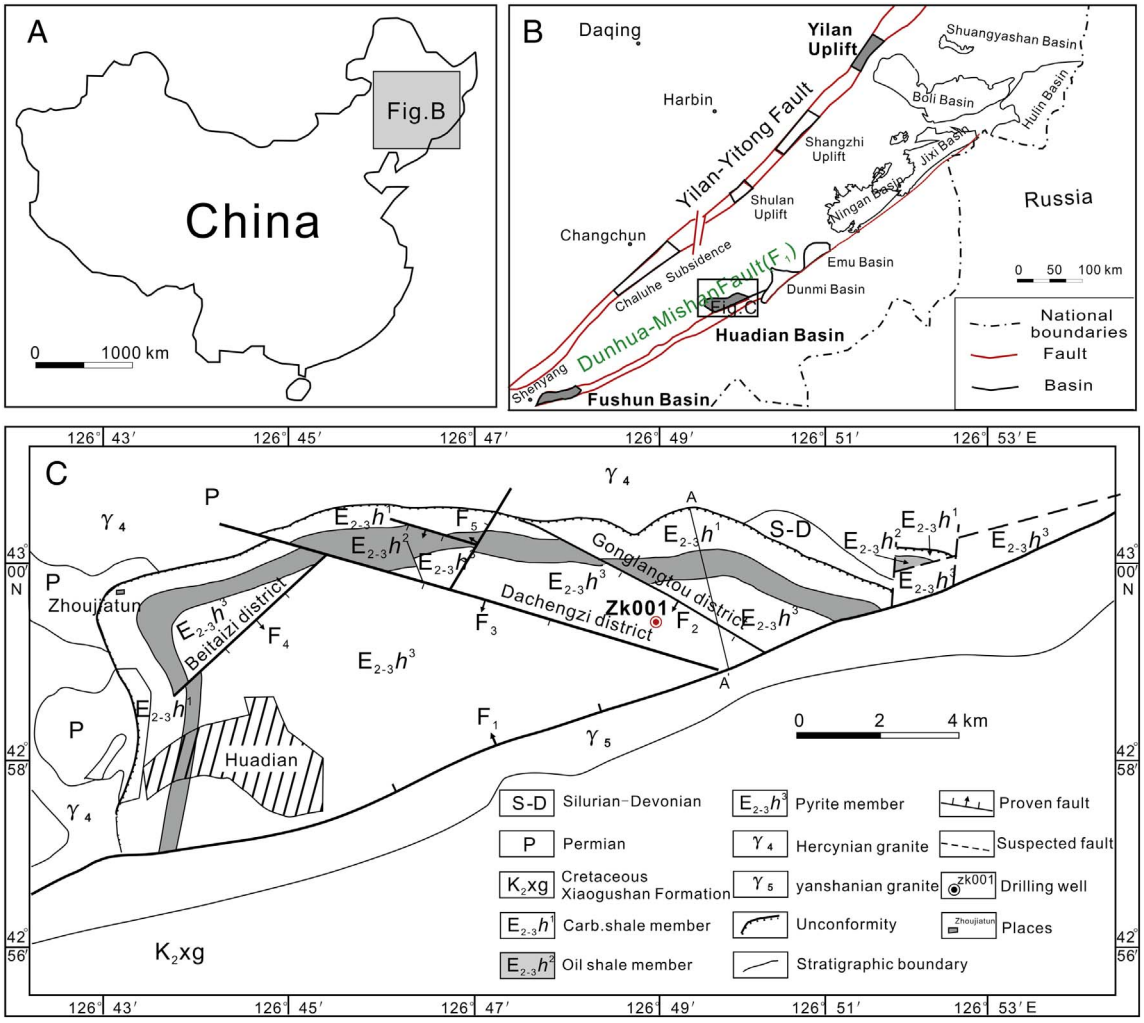

Fig. 1. Geological map of Huadian Basin in Northeast China.

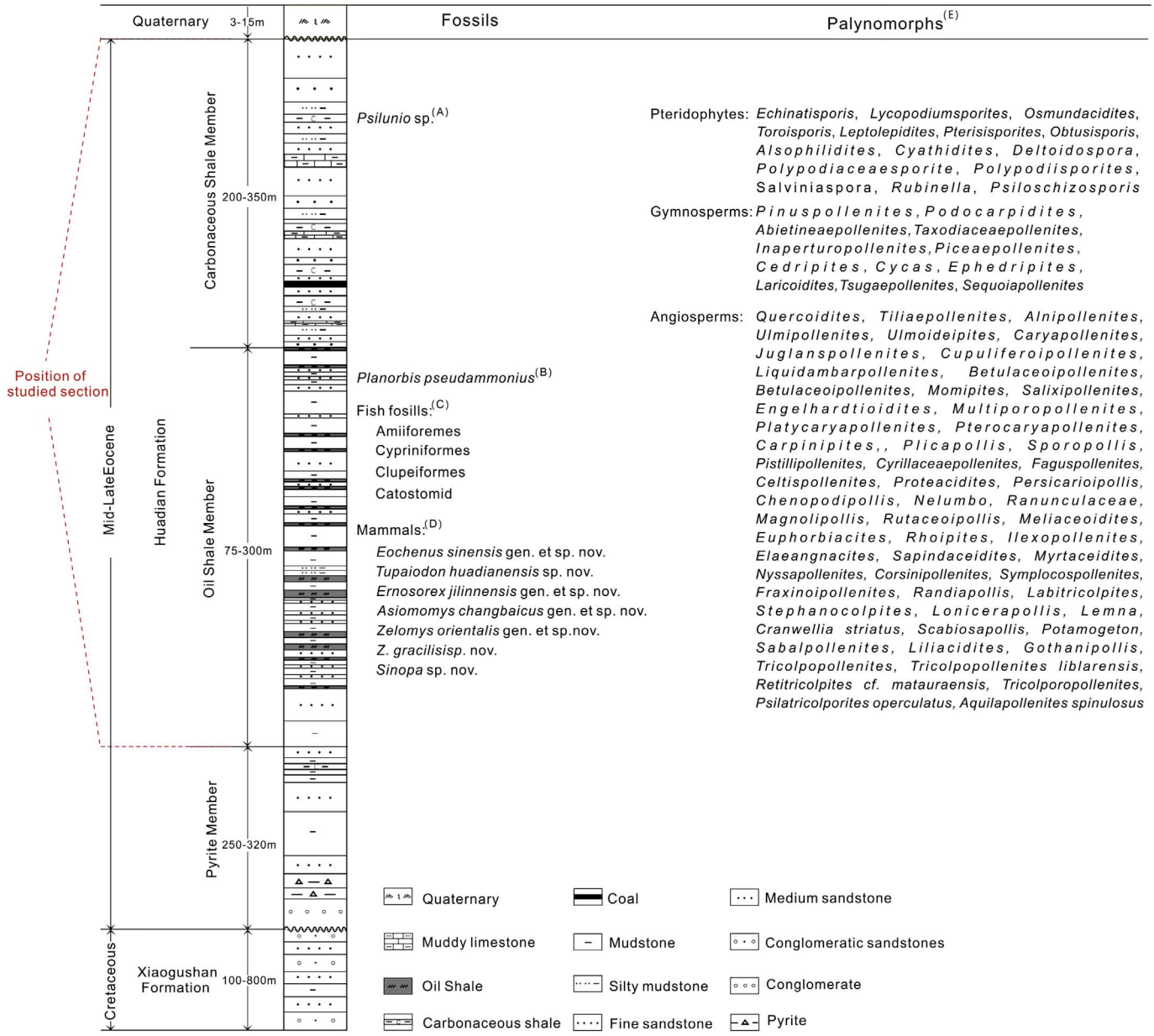
Quaternary
3-15m
Fossils
Palynomorphs(E)
Carbonaceous Shale Member
200-350m
Oil Shale Member
75-300m
Pyrite Member
250-320m
Huadian Formation
Mid-LateEocene
Cretaceous
Xiaogushan Formation
100-800m
Position of studied section
Psilunio sp.(A)
Planorbis pseudammonius(B)
Fish fossils:(C)
Amiiforemes
Cypriniformes
Clupeiformes
Catostomid
Mammals:(D)
Eochenus sinensis gen. et sp. nov.
Tupaiodon huadianensis sp. nov.
Ernosorex jilinnensis gen. et sp. nov.
Asiomomys changbaicus gen. et sp. nov.
Zelomys orientalis gen. et sp.nov.
Z. gracilisisp. nov.
Sinopa sp. nov.
Pteridophytes: Echinatisporis, Lycopodiumsporites, Osmundacidites, Toroisporis, Leptolepidites, Pterisisporites, Obtusisporis, Alsophilidites, Cyathidites, Deltoidospora, Polypodiaceaesporite, Polypodiisporites, Salviniaspora, Rubinella, Psiloschizosporis
Gymnosperms: Pinuspollenites, Podocarpidites, Abietineaepollenites, Taxodiaceaepollenites, Inaperturopollenites, Piceaepollenites, Cedripites, Cycas, Ephedripites, Laricoidites, Tsugaepollenites, Sequoiapollenites
Angiosperms: Quercoidites, Tiliaepollenites, Alnipollenites, Ulmipollenites, Ulmoideipites, Caryapollenites, Juglanspollenites, Cupuliferoipollenites, Liquidambarpollenites, Betulaceoipollenites, Betulaceoipollenites, Momipites, Salixipollenites, Engelhardtioidites, Multiporopollenites, Platycaryapollenites, Pterocaryapollenites, Carpinipites,, Plicapollis, Sporopollis, Pistillipollenites, Cyrillaceaepollenites, Faguspollenites, Celtispollenites, Proteacidites, Persicarioipollis, Chenopodipollis, Nelumbo, Ranunculaceae, Magnolipollis, Rutaceoipollis, Meliaceoidites, Euphorbiacites, Rhoipites, Ilexopollenites, Elaeangnacites, Sapindaceidites, Myrtaceidites, Nyssapollenites, Corsinipollenites, Symplocospollenites, Fraxinoipollenites, Randiapollis, Labitricolpites, Stephanocolpites, Lonicerapollis, Lemna, Cranwellia striatus, Scabiosapollis, Potamogeton, Sabalpollenites, Liliacidites, Gothanipollis, Tricolpopollenites, Tricolpopollenites liblarensis, Retitricolpites cf. matauraensis, Tricolporopollenites, Psilatricolporites operculatus, Aquilapollenites spinulosus
Quaternary
Muddy limestone
Oil Shale
Carbonaceous shale
Coal
Mudstone
Silty mudstone
Fine sandstone
Medium sandstone
Conglomeratic sandstones
Conglomerate
Pyrite

Fig. 2. Comprehensive sedimentary succession and biostratigraphy of Huadian Formation in the Huadian Basin. A and B - based from Bureau of Geology and Mineral Resources of Jilin Province (1988); C - based from Zhou and Sun (1985), Liu and Chang (2009); D - based from Wang and Li (1990); E - based on the study results in this paper.

Huadian Basin during the Middle to Late Eocene, based on a continuous 505 m long drill core. We focus particularly on seasonal variations in paleoclimate, their connections with the East Asian Monsoon, and their implications for oil shale formation. We compare our paleoclimatic results with those from other parts of northeastern China (including the Fushun Basin in Liaoning, the Huadian, Huchun and Jishu basins in Jilin, and the Yilan Basin in Heilongjiang Province), as well as with other Middle Eocene studies from North America and Europe, in order to explore possible global climatic changes during the Middle and Late Eocene.

2. Geologic setting of the Huadian Basin

Several oil shale- and coal-bearing basins are located in the Dunhua-Mishan Fault Zone of northeastern China (Liu et al., 2009; Fig. 1B), with the most prominent of these units located in the Huadian and Fushun basins. The Huadian Basin, a small, fault-controlled strike-slip basin, is located in the middle part of the Dunmi Fault Zone, which trended to the NE during the Paleogene (Panel F_1 in Fig. 1C). The basin fill (i.e., the Huadian Formation) is up to 1500 m thick and directly overlies various basement units including granites as well as lower Paleozoic and Permo-Carboniferous sedimentary rocks. Huadian Formation outcrops are rare, due to Quaternary cover up to 15 m thick (Sun et al., 2013). The Huadian Formation consists of a lower Pyrite Member ($E_{2-3}\,h^1$), a middle Oil Shale Member ($E_{2-3}\,h^2$), and an upper Carbonaceous Shale Member ($E_{2-3}\,h^1$) (Fig. 2).

The Pyrite Member was deposited during the initial subsidence of the basin, in a shallow lake of limited areal extent. This unit is predominantly composed of gray mudstone, intercalated with thin layers of sandstone. It contains locally recoverable pyrite layers, as well as brick red, purple, and green mudstones. The Oil Shale Member was deposited during the stage of maximum basin subsidence, which expanded and deepened the Huadian depositional lake. These sediments are mainly composed of gray to dark gray mudstones and oil shales, intercalated with thin layers of gray to white fine sandstone. The Carbonaceous Shale Member formed during the final stage of Huadian

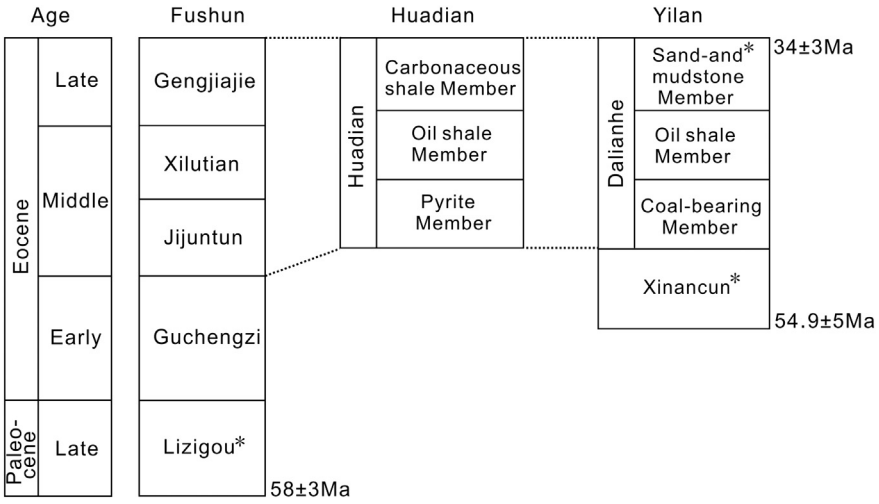

Fig. 3. Stratigraphic correlation of Eocene between Fushun, Huadian and Yilan Basin. Asterisks indicate formation with geochemical dating: lower part of Lizigou formation of Fushun-58.0 ± 3 Ma (zircon fission track dating; Quan et al., 2012); lower part of Xinancun formation and the upper part of Dalianhe formation of Yilan-54.9 ± 5 Ma and 34 ± 3 Ma (zircon fission track dating; Huang et al., 1998; Yang et al., 2004; Zhang et al., 2007).

Basin subsidence. It mainly consists of gray mudstone, black carbonaceous shale, coal, and gray to white, fine to coarse sandstone (Sun et al., 2013).

Despite the lack of published geochronological data, the age of the Huadian Formation can be reliably constrained based on paleontological evidence, including palynomorphs and macrobotanical remains as well as mammal, bird, reptile, and fish fossils (Zhou and Sun, 1985; Bureau of Geology and Mineral Resources of Jilin Province, 1988; Wang and Li, 1990; Manchester et al. 2005; Liu and Chang, 2009; Smith et al. 2011; Fig. 2). Further age constraint comes from lithostratigraphic correlation with the oil shale- and coal-bearing layers of the well-dated Fushun and Yilan basins (Huang et al., 1998; Yang et al., 2004; Zhang et al., 2007; Meng, 2010; Quan et al., 2012); the Huadian Formation is equivalent to the Jijuntun, Xilutian, and Gengjiajie formations of the Fushun Basin and the Dalianhe Formation of the Yilan Basin (Fig. 3). These analyses indicate that the Huadian Formation is Middle to Late Eocene in age (hereafter referred to as mid-late Eocene).

3. Materials and methods

We collected a total of 99 palynological samples for this study, from 25.3 m to 505 m depth in a drill core from Well ZK001, located in the southeastern Huadian Basin (Fig. 1C). Of these samples, 53 come from the Carbonaceous Shale Member, which ranges from 25.3 to 331.7 m in depth in Well ZK001; the remaining 46 samples are from the Oil Shale Member, which ranges in depth from 331.7 to 505 m (Fig. 4). This continuous lithological record of the Huadian Formation allows us to study climatic and environmental change during the Middle and Late Eocene.

All samples were prepared and identified at the Research Center of Paleontology and Stratigraphy, at Jilin University in Changchun, China. The preparation process is as follows: 30 g of sifted dry sample was first treated with hydrochloric acid, followed by hydrofluoric acid, then another round of hydrochloric acid. The residue was then sieved with a 6 μm mesh size, and mounted on slides with glycerine gelatine for identification under a microscope.

Most of the samples provided sufficient numbers of palynomorphs and organic matter. Out of the 99 total samples, in 8 samples we counted at least 250 palynomorph grains, 76 samples provided > 200 palynomorph grains, and only 15 samples show < 200 palynomorph grains. Palynological diagrams were created using the TILIA and TiliaGraph programs, and palynological zones were distinguished using CONISS software (Grimm, 2011).

The paleoclimatic analysis employed in this study follows the Coexistence Approach (CA; Mosbrugger and Utescher, 1997; Utescher et al., 2014). This method is one of the Nearest Living Relative (NLR) techniques, and relies on the assumption that since the late Paleogene the climatic requirements of plant taxa have remained similar to those of their nearest living relatives. With the Coexistence Approach, the climatic ranges in which a maximum number of NLRs of a given fossil flora can coexist is determined independently for each climate parameter analyzed, and is considered to be the best analogue for the paleoclimate at the time of deposition.

The Coexistence Approach can be applied using the ClimStat computer program and the Palaeoflora database (www.palaeoflora.de), which contains climatic information on > 1600 extant plant taxa. Typically, the resolution and reliability of the coexistence intervals increases an increasing number of taxa included in the analysis, especially when the flora contains with ten or more taxa for which climate parameters are known. The accuracy of the calculated climate parameters varies, with temperature-related parameters usually accurate to within 1–2 °C. Mean annual precipitation (MAP) results are accurate to within 100–200 mm; other precipitation parameters are less precise, but are likely to accurately reflect overall temporal trends (Mosbrugger and Utescher, 1997; Utescher et al., 2014).

The Coexistence Approach has been used to estimate paleoclimatic parameters from Palaeogene and Neogene fossil floras in Europe (Ivanov et al., 2002, 2007; Uhl et al., 2003; Roth-Nebelsick et al., 2004; Feurdean et al., 2008; Utescher and Mosbrugger, 2007, Utescher et al., 2011a, Utescher et al., 2011b; Bruch and Mosbrugger, 2002, Bruch et al., 2011) and East Asia, especially in China (e.g., Liang et al., 2001, 2003; Yang et al., 2002; Zhao et al., 2004; Kou et al., 2006; Xu et al., 2008; Xia et al., 2009; Yao et al., 2009; Hao et al., 2010; Wang et al., 2010; Meng et al., 2012a, b; Quan et al., 2012). In this study, we estimated seven climatic parameters, including mean annual temperature (MAT), mean temperature of the warmest month (WMT), mean temperature of the coldest month (CMT), mean annual precipitation (MAP), precipitation of the wettest month (HMP), precipitation of the driest month (LMP), and precipitation of the warmest month (WMP).

4. Results and interpretation

4.1. Palynological zones

In total, 85 palynomorph genera and 100 palynomorph species were identified in this study. These morpho-taxa include 15 genera of ferns, 12 genera of gymnosperms, and 58 genera of angiosperms. Some selected spores and pollen recovered from the Huadian Formation are shown in Fig. 5. The gymnosperm assemblage is dominated by pollen with air sacs; abundant taxa include *Pinuspollenites* (maximum abundance of 55.0%), *Podocarpidites* (39.5%), *Abietineaepollenites* (30.0%), *Taxodiaceaepollenites* (23.0%) and *Inaperturopollenites* (13.5%). The

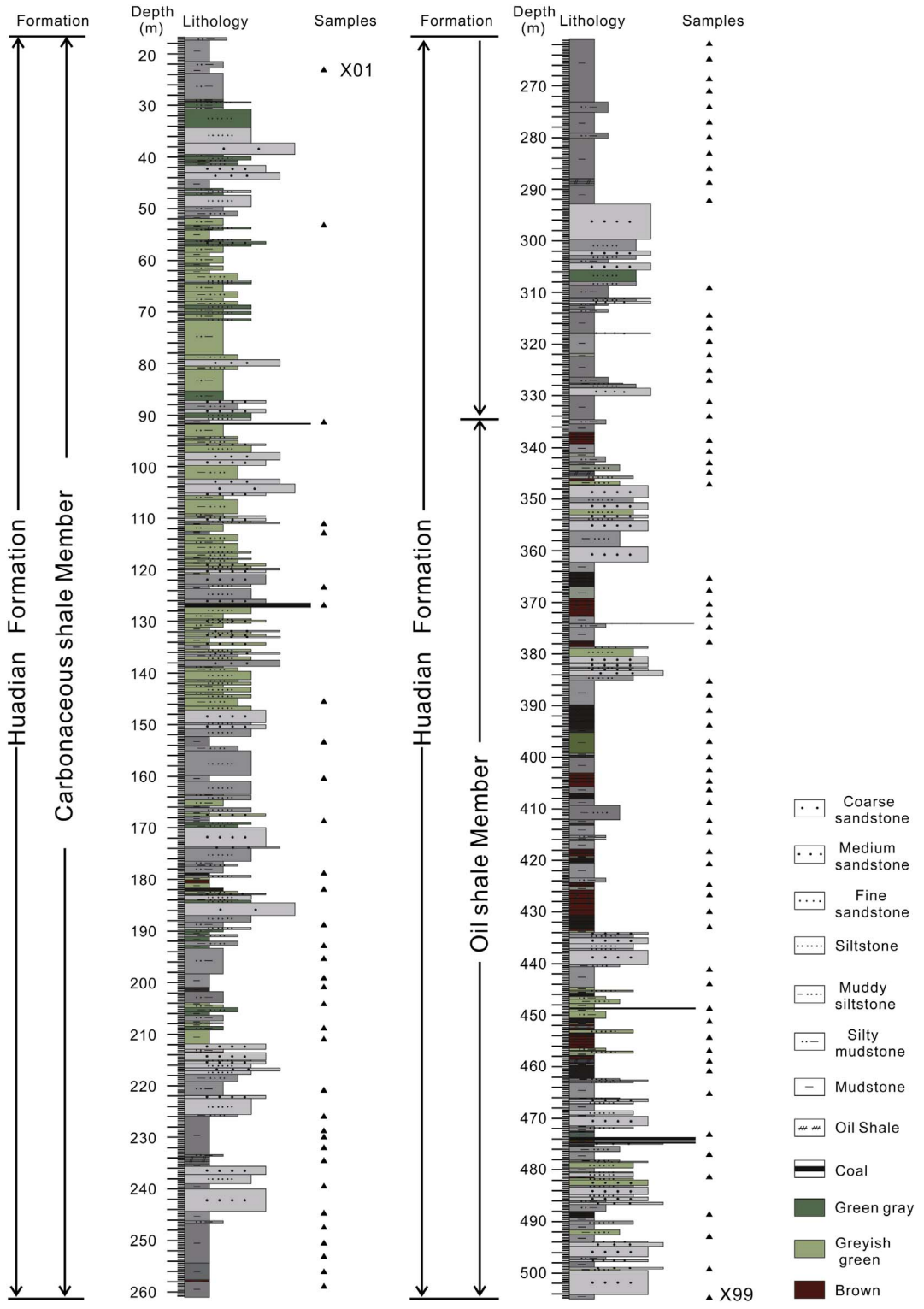

Fig. 4. Sampling locations of Huadian Formation in Well ZK001, Huadian Basin.

angiosperm assemblage mainly comprises *Quercoidites* (61.0%), *Tiliaepollenites* (39.0%), *Alnipollenites* (35.5%), *Ulmipollenites* (22.5%), *Liquidambarpollenites* (19.5%), *Ulmoideipites* (19.5%), *Cupuliferoipollenites* (15.0%), *Juglanspollenites* (14.5%) and *Betulaceoipollenites* (10.0%). Other pollen taxa are rare or occur sporadically.

The morpho-taxa of this palynoflora can be assigned to Nearest Living Relatives (NLRs) which in turn provide information on the bioclimatical preferences of the different elements in China. Thus, 30 taxa relate to mainly subtropical plants (accounting for 35.3% of the total assemblage), i.e., *Pterisisporites*, *Taxodiaceaepollenites*, *Ilexopollenites*, *Myrtaceidites*, etc.; 12 taxa are assigned to subtropical-temperate plants (14.1% of the total assemblage), i.e., *Euphorbiacites*, *Fraxinoipollenites*, *Ulmipollenites*, *Abietineaepollenites*, etc.; and 20 taxa related to mainly temperate plants (23.5% of the total assemblage), i.e., *Ephedripites*, *Cupuliferoipollenites*, *Betulaceoipollenites*, etc. There are also 15 morphotaxa with NLRs having a global distribution, and 8 are of unknown

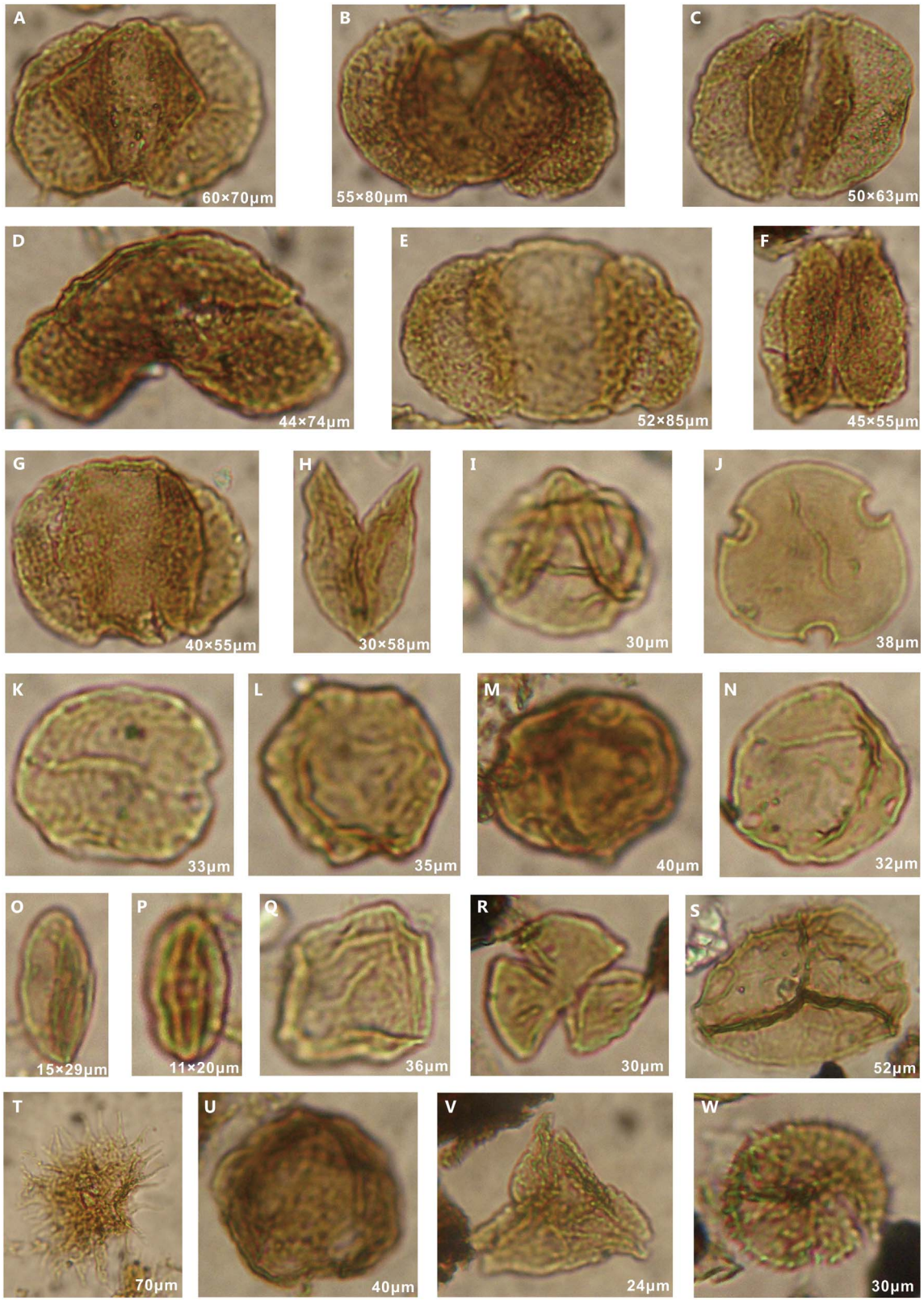

Fig. 5. A selection of the spores and pollen discovered from the Huadian Basin.
A–C *Podocarpidites*, D–E *Pinuspollenites*, F–G *Abietineaepollenites*, H - *Taxodiaceaepollenites*, I - *Inaperturopollenites*, J- *Tiliaepollenites*, K - *Ulmipollenites*, L - *Pterocarya*, M - *Liquidambarpollenites*, N - *Caryapollenites*, O - *Quercoidites microhenrici*, P-oval *Cupuliferoipollenites*, Q - *Ulmoideipiteskrempii*, R - Ranunculaceae, S - *Lycopodiumsporites* T - *Pediastrum*, U - *Concentricystes*, V - *Potamogeton*, W - *Lemna*.

affinity (Table S-1). In general, this points to a mid-late Eocene flora dominated by elements of subtropical evergreen and deciduous broad-leaved forests.

Cluster analysis yields 4 palynozones in the Huadian Formation (Fig. 6). Zones I and II make up the Oil Shale Member, and while Zones III and IV make up the Carbonaceous Shale Member. The features of

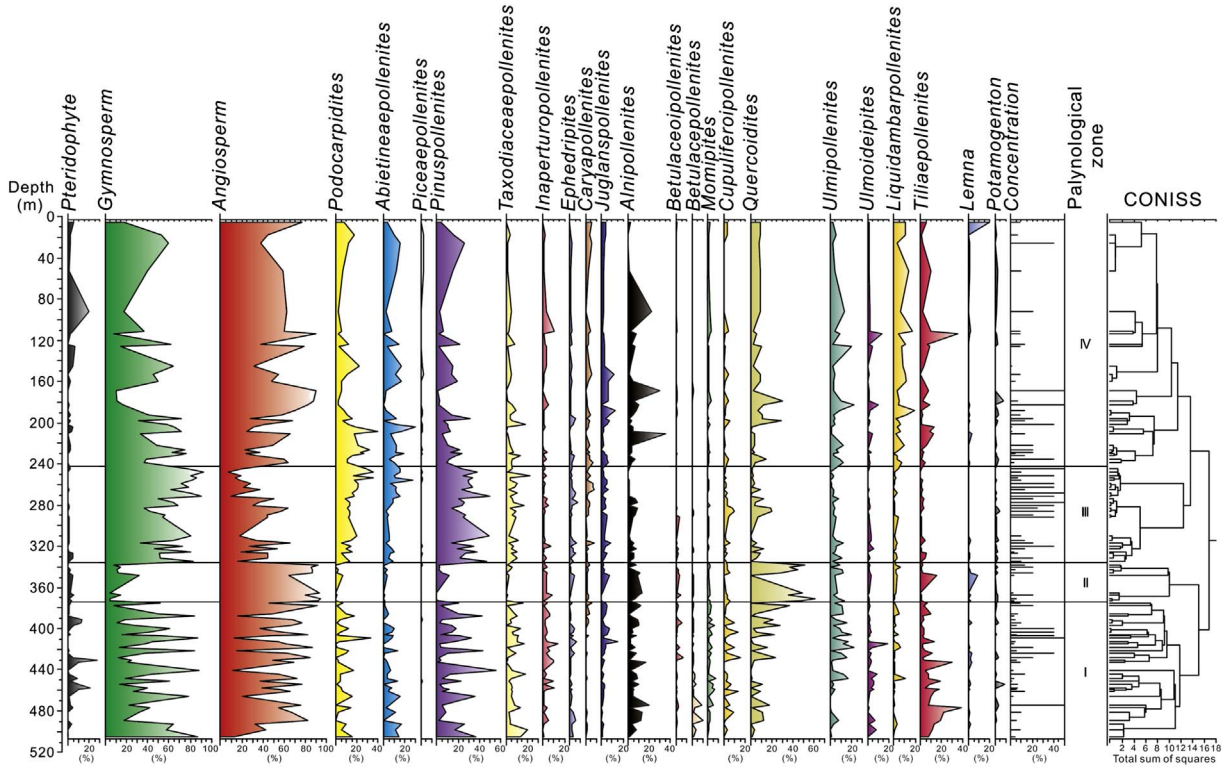

Fig. 6. Pollendiagram of percentages of Eocene Huadian Formation including the main types of pollen and spores. The diagram at the right shows the results of CONISS cluster analysis, which is the basis for pollen zonation.

each zone are described below:

4.1.1. Zone I

Zone I ranges from 505 to 374 m in depth. It includes 70 palynomorph taxa, including 49 angiosperms, 11 gymnosperms, and 10 ferns. Gymnosperm (8.0–88.0%) and angiosperm (12.0–91.0%) taxa alternately dominate the assemblage. The gymnosperm taxa (mostly evergreens) include *Pinuspollenites*, *Taxodiaceaepollenites* and *Abietineaepollenites*, representing plant communities that are now found in both subtropical and temperate regions. A high percentage of *Podocarpidites* (1.0 to 32.8%), a subtropical to tropical taxon, is also present in the assemblage. Angiosperm palynomorphs include *Tiliaepollenites*, *Quercoidites*, *Ulmipollenites*, *Alnipollenites,* and *Ulmoideipites*, and are derived mostly from evergreen or deciduous broad-leaved trees and shrubs that now grow in subtropical and temperate regions. Fern spores are less common (0.4 to 27.5%), and include *Alsophilidites*, *Deltoidospora*, *Polypodiaceaaesporites*, *Cyathidites*, and *Toroisporis*. A few aquatic algae such as *Pediastrum* and *Lemna* also occur in this zone.

4.1.2. Zone II

Zone II ranges from 374 to 336 m in depth. It contains 48 palynomorph taxa, including 10 gymnosperms, 31 angiosperms, and 7 ferns. Unlike Zone I, the assemblage is dominated by angiosperm pollen (64.4 to 94.0%), which mostly reflect evergreen or deciduous broad-leaved trees or shrubs. The assemblage is dominated by taxa that now grow in subtropical and temperate regions; *Quercoidites* is the most common palynomorph, but *Alnipollenites* and *Ulmipollenites* are also present in high abundances. A few tropical and subtropical taxa, such as *Caryapollenites* and *Liquidambarpollenites,* are also present, along with some temperate deciduous tree taxa such as *Cupuliferoipollenites*, *Tiliaepollenites,* and *Juglanspollenites*. Gymnosperm taxa account for 5.0 to 31.6% of total palynomorphs, with the assemblage dominated by *Pinuspollenites*, *Inaperturopollenites*, *Podocarpidites,* and *Taxodiaceaepollenites*. Fern spores are relatively rare (1.0 to 6.0%), represented by a few specimens of *Polypodiaceaaesporites* and *Osmundacidites*.

4.1.3. Zone III

Zone III ranges from 336 to 242 m in depth. In total, 62 palynomorphs taxa occur in this zone, comprising 11 gymnosperms, 41 angiosperms, and 10 ferns. Like Zone I, evergreen gymnosperm taxa dominate this assemblage, ranging from 33.5 to 92.5% of total palynomorphs. They are represented mainly by *Pinuspollenites* (13.6 to 47.0%), with smaller proportions of *Abietineaepollenites* and *Taxodiaceaepollenites*. The subtropical to tropical taxon *Podocarpidites* is also present in relatively high abundances (5.0 to 35.0%). Angiosperm taxa occur at a lower frequency (7.5 to 65.5%) than in Zone II, and are represented by subtropical to temperate taxa such as *Quercoidites*, *Ulmipollenites*, *Cupuliferoipollenites,* and *Alnipollenites*. A relatively low proportion of fern spores (0.4 to 4.0%), e.g., *Osmundacidites*, *Polypodiaceaesporite*, *Obtusisporis*, is present in this zone.

4.1.4. Zone IV

Zone IV ranges from 242 to 17.9 m in depth. This zone contains 66 palynomorph taxa, including 48 angiosperms, 10 gymnosperms, and 8 ferns. Angiosperm pollen dominates the assemblage, ranging from 22.5 to 90.0% of the total pollen sum, and reflects the presence of evergreen and deciduous broad-leaved trees such as *Quercoidites*, *Ulmipollenites*, *Tiliaepollenites*, *Alnipollenites*, and *Liquidambarpollenites*. Gymnosperm palynomorphs (7.5 to 76.0%) occur at a lower frequency than in Zone III, and include abundant *Podocarpidites*, *Pinuspollenites,* and *Abietineaepollenites*. Fern spores are sporadically present in this zone (0.5 to 20.0%) and include *Polypodiaceaesporite*, *Lycopodiumsporites*, *Toroisporis*, and *Osmundacidites*.

4.2. Climatic reconstruction

Our CA climate reconstruction is based on 86 fossil palynomorph taxa and their Nearest Living Relatives, as shown in Table S-2. Seven paleoclimatic parameters (MAT, WMT, CMT, MAP, HMP, LMP and

WMP) were calculated for each sample from the two members of the Huadian Formation. These results are shown in Figs. 7 and 8. Additionally, palynomorph assemblages from single samples were combined based on their assignment to one of the two lithostratigraphic members, and to the four palynozones. The CA results from these combined samples are reported in Table 1 and shown in Fig. 9.

In the Oil Shale Member (Table 1, Figs. 7 and 9), the combination of all samples yields the following paleoclimate values: MAT ranges from 16.5 to 18.4 °C (mean = 17.45 °C); CMT ranges from 6.6 to 7.8 °C (mean = 7.2 °C); WMT ranges from 27.3 to 27.9 °C (mean = 27.6 °C); MAP ranges from 1035 to 1206 mm (mean = 1120.5 mm); HMP ranges from 204 to 236 mm (mean = 220 mm); LMP ranges from 16 to 41 mm (mean = 28.5 mm); WMP ranges from 55 to 61 mm (mean = 58 mm) and 99 to 143 (mean = 121 mm). In the Carbonaceous Shale Member (Table 1, Figs. 8 and 9), the combination of all samples yield the following values: MAT ranges from 13.6 to 16.1 °C (mean = 14.85 °C); CMT ranges from 5.5 to 7.8 °C (mean = 6.65 °C); WMT ranges from 23.6 to 25.6 °C (mean = 24.6 °C); MAP ranges from 887 to 1206 mm (mean = 1046.5 mm); HMP ranges from 187 to 236 mm (mean = 211.5 mm); LMP ranges from 16 to 41 mm (mean = 28.5 mm); WMP ranges from 45 to 61 mm (mean = 53 mm). Comparing the paleoclimatic reconstructions from the two data sets, it is evident that the values of six parameters (MAT, CMT, WMT, MAP, HMP, and WMP) are higher in the Oil Shale Member than in the Carbonaceous Shale Member, recording a general decrease in temperature and precipitation (Table 1; Figs. 9A and B).

The climatic parameters calculated from each of the four palynological zones (Table 1; Figs. 9C–F) yield trends in MAT, MWT, LMP, and WMP similar to those described above (Table 1; Figs. 9A and B). However, palynological zones II and III yield slightly wider coexistence intervals for CMT, MAP and HMP, and CMT increases clearly in zones II and III before decreasing towards Zone IV. MAP and HMP also increase in Zone II, but decrease in zones III and IV, following the general trend.

5. Discussion

5.1. Comparison of palynoflora and paleoclimate with other records from northeastern China

The quantitative results presented in this study suggest that the Middle to Late Eocene climate of the Huadian Basin was warm and humid, with a MAT of at least 13.6 °C and a MAP of > 887 mm. Consistent trends in climatic parameters clearly reflect cooling and drying of climate during the transition from the Oil Shale Member to the Carbonaceous Shale Member in the mid-late Eocene. The transition to an "icehouse" climate in the late Eocene to early Oligocene had been well established based on marine proxy data (Dall'Antonia et al., 2003; Persico and Villa, 2004; Abelson et al., 2008; Bijl et al., 2009; Houben et al., 2012) and continental sedimentary records, mostly from North America, Australia, and Europe (Wolfe, 1993; Prothero and Berggren, 1992; Ivany et al., 2000). The results presented in this study provide evidence for climatic cooling in the mid-late Eocene, from a continental sedimentary succession in northeastern China.

Several similar environmental settings are represented in this region which served for studies on paleo-lake sedimentary environments (Liu et al., 2012; Xu et al., 2012; Meng et al., 2012a, b; 2013; Sun et al., 2013; Bai et al., 2015). Especially the Fushun Basin is a well-known and well-studied example. The Fushun Basin, in Liaoning Provnice, northeastern China, is a typical Cenozoic fault basin located in the western Dunhua-Mishan Fault Zone. It is an important site for coal and oil shale production (Fig. 1B). The Eocene palynoflora and paleoclimate of the Fushun Basin have been studied in great detail (Hong et al., 1980; Shi et al., 2008; Wang et al., 2010; Meng et al., 2012a, b; Quan et al., 2012), allowing for direct comparison with those of the Huadian Basin.

The Middle Eocene succession in the Fushun Basin is represented mainly by the Jijuntun and Xilutian formations, and is quite similar to the Huadian Basin succession in terms of its palynoflora and plaeoclimate characteristics. The Jijuntun Formation is conformably overlain by the Xilutian Formation, and the pollen assemblages of both units are quite similar. Both palynomorph assemblages are dominated by angiosperm pollen (> 80%); *Quercoidites* is the most abundant taxon, with an average content of 46% and a maximum of 60%; *Ulmipollenites* is also present in high abundances. Gymnosperm pollen represents 5 to 16% of total palynomorphs, and are dominated by *Taxodiaceaepollenites* and *Pitysporites*. Fern spores are rare (Hong et al., 1980).

Of the 46 palynomorph taxa recovered from the Jijuntun and Xilutian formations in the Fushun Basin (Wang et al., 2010), 32 taxa are also found in the Huadian Basin. Within the Middle Eocene palynoflora of the Fushun Basin, 43.8% of palynomorphs show tropical-subtropical features, including *Cedripites*, *Podocarpidites*, *Caryapollenites*, *Cyrillaceaepollenites*, *Engelhardtioipollenites*, *Liquidambarpollenites*, *Palmaepollenites*, *Platycarya*, *Rhoipites*, and *Rutaceoipollenites*. Another 18.8% show subtropical to temperate features, including *Quercoidites*, *Ulmipollenites*, *Pinuspollenites*, *Taxodiaceaepollenites*, *Alnipollenites*, and *Fraxinoipollenites*. Overall, the Middle Eocene palynoflora of the Fushun Basin indicates a generally subtropical climate.

The Middle Eocene paleoclimate of the Fushun Basin has been quantitatively reconstructed using the CA (Wang et al., 2010; Meng et al., 2012a, b and Quan et al., 2012). Differences in sampling strategy between the various studies has led to slight differences in the calculated MAP and MAT, however, the data clearly reveal a climate characterized by a high annual average temperature (average MAT ≥ 13.6 °C) and abundant rainfall (average MAP ≥ 1048.5 mm). Quan et al. (2012) compared the temperature evolution of the Eocene Fushun Basin with the marine oxygen isotope record, identifying an Early Eocene warming trend, followed by a cooling trend at ca. 43–45 Ma and subsequent warming in the late Middle Eocene. The Middle Eocene cooling trend apparent in our data from the Huadian Basin seems to reflect this pattern.

Other Eocene records from northeastern China show similar climatic signals. In the Hunchun Basin, MAT and MAP during the mid-late Eocene were reported as 14.3–14.9 °C and 797.5–1344 mm, respectively (Kou, 2005). However, these values are estimated from the entire succession, so no temporal changes can be recognized. The mid-late Eocene succession of the Dalianhe Basin yields a MAT of 20.6–20.8 °C in the Lower Member (Middle Eocene), which then fell to 13.3–15.6 °C during a Middle Eocene cooling trend, followed by an increase to 15.7–18.4 °C in the Upper Member (Late Eocene). This pattern, with a cooler phase in the Middle Eocene, agrees well with our Huadian results. Moreover, MAP in the Lower Member was approximately 1122–1362 mm, which decreased to 979–1281 mm before increasing again to 1304–1355 mm in the Upper Member (Quan et al., 2012). In the Middle Eocene of the Jishu Basin, MAT was around 15.6–18.4 °C and MAP was 897–1206 mm (Quan et al., 2012). The similarity of climatic data from the various basins suggests that the mid-late Eocene climate of northeastern China was consistently warm and humid; additionally, a cooler phase within the Middle Eocene is observed in most basins.

5.2. Comparison with contemporaneous sites from North America and Europe

Quantitative paleoclimatic data from the Huadian Basin can be compared with mid-late Eocene records from North America and Europe. The Middle Eocene climate of southwestern Wyoming (USA) was assessed using the leaf morphology and taxonomic affinities of plant macrofossils; the MAT was determined to be 12–21 °C, with MAP of 800–1500 mm (Wing et al., 1999; Wang et al., 2010). In a Middle Eocene succession in Oregon, the MAT calculated by leaf margin analysis (LMA) was 14–17 °C (Manchester, 2000). In the Middle Eocene succession of Messel, Germany, the MAT calculated via LMA is approximately 22 °C (up to ~ 24 °C), while the MAP calculated by CA was

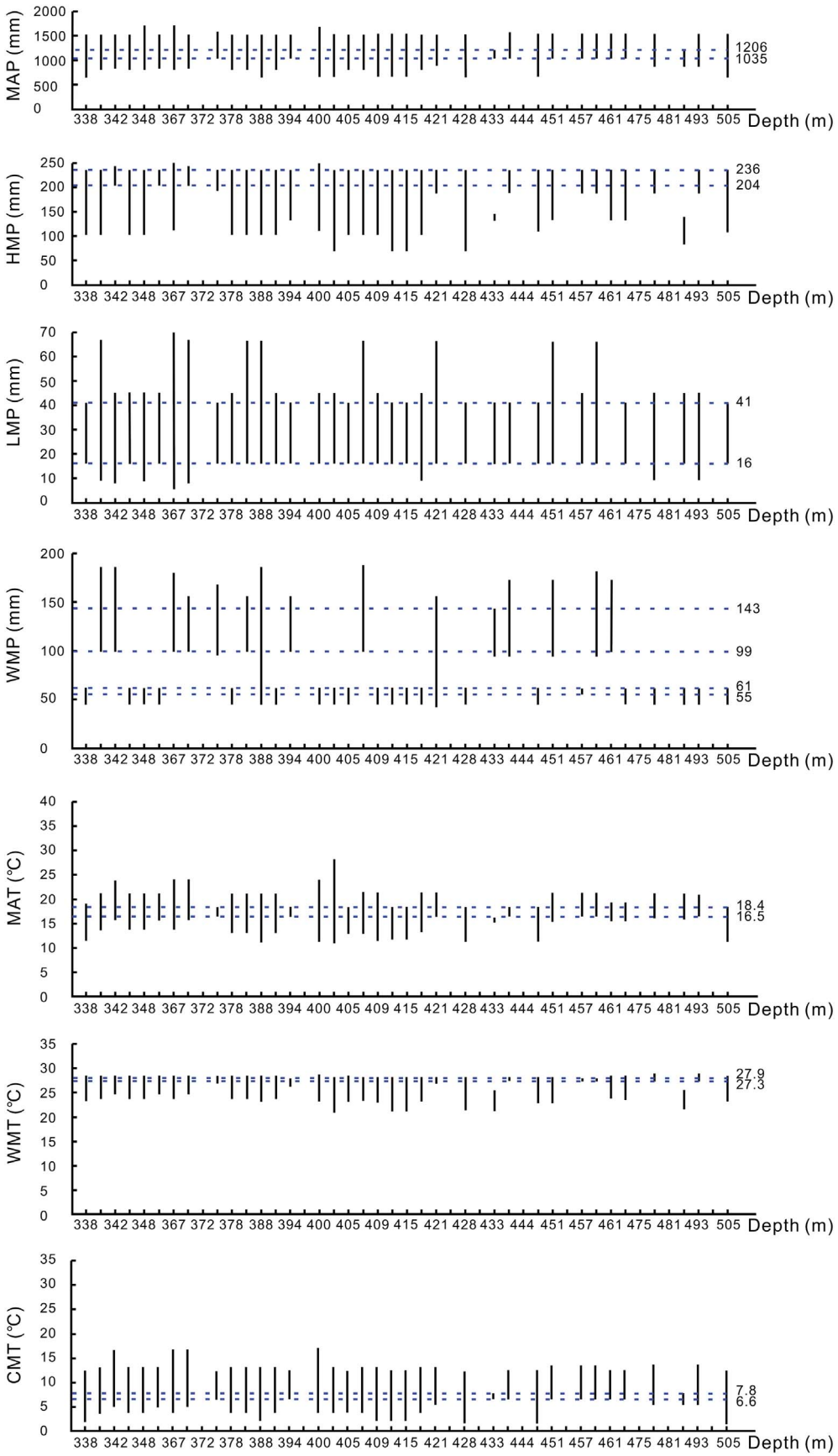

Fig. 7. Climatic coexistence intervals of 55 samples in the middle Oil Shale Member of Huadian Formation.

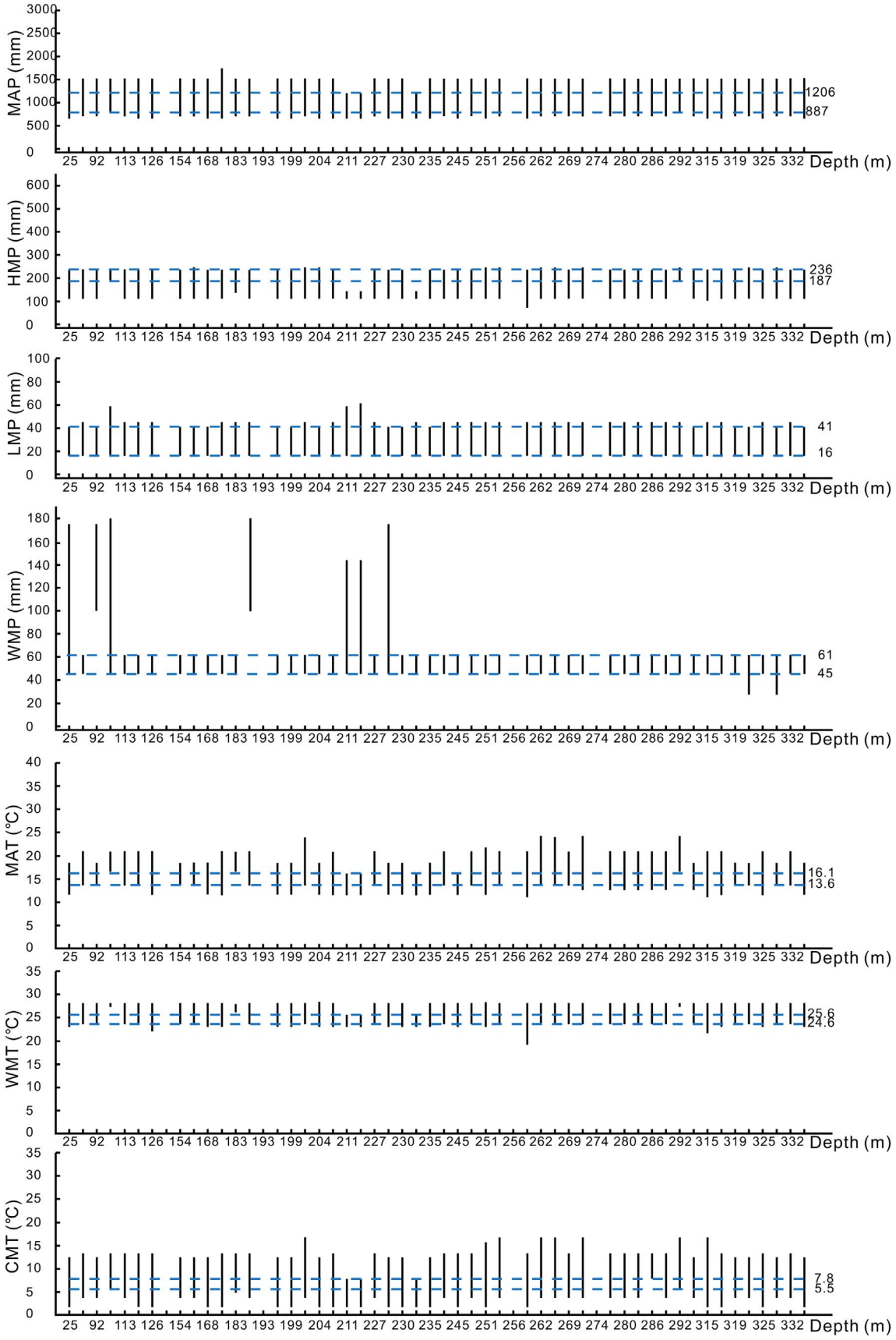

Fig. 8. Climatic coexistence intervals of 54 samples in the upper Carbonaceous Shale Member of Huadian Formation.

Table 1
Palaeoclimatic results of CA analysis for the two mid-late Eocene members of Huadian Basin and each palynological zone, with mean values in brackets.

Palynological zone	Depth (m)	MAT (°C)	WMT (°C)	CMT (°C)	MAP (mm)	HMP mm)	LMP (mm)	WMP (mm)
Carbonaceous Shale Member	5.2–336	13.6–16.1 (14.9)	23.6–25.6 (24.6)	5.5–7.8 (6.7)	887–1206 (1047)	187–236 (212)	16–41 (29)	45–61 (53)
Oil Shale Member	336–505	16.5–18.4 (17.5)	27.3–27.9 (27.6)	6.6–7.8 (7.2)	1035–1206 (1121)	204–236 (220)	16–41 (29)	55–61 (58), 99–143 (121)
Zone IV	17.9–242	13.6–16.1 (14.9)	23.6–25.6 (24.6)	5.5–7.8 (6.7)	887–1206 (1047)	187–236 (212)	16–41 (29)	45–61 (53)
Zone III	242–336	13.6–18.4 (16.0)	27.3–28.1 (27.7)	7.8–12.5 (10.2)	887–1520 (1204)	187–236 (212)	16–41 (29)	45–61 (53)
Zone II	336–374	16.5–18.4 (17.5)	27.3–28.1 (27.7)	6.6–12.5 (9.6)	1035–1520 (1278)	204–236 (220)	16–41 (29)	45–61 (53), 99–154 (127)
Zone I	374–505	16.5–18.4 (17.5)	27.3–27.9 (27.6)	6.6–7.8 (7.2)	1035–1206 (1121)	187–236 (212)	16–41 (29)	55–61 (58), 99–143 (121)

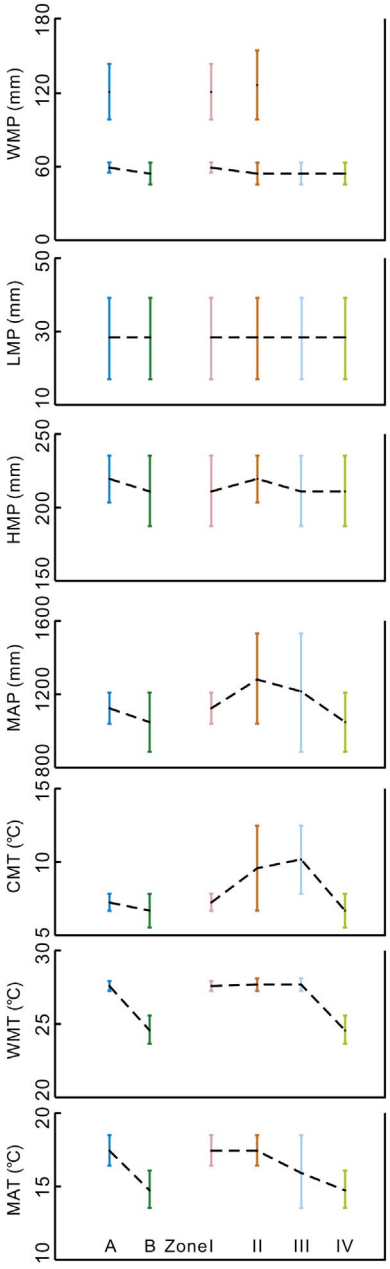

Fig. 9. Coexistence intervals of the Huadian Formation and each of the four palynological zones. A - Oil Shale Member; B - Carbonaceous Shale Member.

approximately 2500 mm and the mean relative air humidity was 77%. Both CA and LMA suggest a warm, humid, frost-free climate (Grein et al., 2011). In the Artemo-Tavrichanskii Basin of Southern Primory'e, Russia, the highest MATs of the Middle Eocene calculated by CA was recorded in the Lutetian as 17–21 °C, while MAP was 1200–1400 mm (Utescher et al., 2015). In the Weisselster and Lausitz basins of northern Germany, the MAT was 23–25 °C in the Middle Eocene, which then declined to 16–21 °C in the Bartonian, followed by a brief warming trend and another decrease to 16–20 °C by the end of Eocene. MAP was approximately 1000–1600 mm, increasing to 1400–1600 mm before decreasing to 1100–1300 mm at the end of the Eocene (Mosbrugger et al., 2005; Utescher et al., 2015; Wang et al., 2010).

In summary, these data indicate that MAT and MAP values from northeastern China during the mid-late Eocene are similar to those from North America, but slightly lower than the European ones. This climatic differentiation is most likely due to the fact that the paleogeographic positions of the relevant middle Eocene sites in Europe are slightly further south than those of the North American, Russian and Chinese sites (Fig. 10). This may confirm a low but detectable latitudinal climatic gradient in the Northern Hemisphere (Utescher et al., 2011b, 2015).

On the other hand, the European sites are located in the west of the Eurasian continent, close to the large water bodies of the North Atlantic Ocean and the Tethys Ocean (Fig. 10). This position under oceanic climate conditions points to a generally equable and very humid climate and may as well as account for the observed differences to the other sites. Furthermore, the region is supposed to be already affected by the Gulf Stream, including its eastern extension, the North Atlantic Current (NAC) (e.g. Wade et al., 2003; Via and Thomas, 2006; Krapp and Jungclaus, 2011). The presence of an effective Paleo-Gulf Stream analogue during the Middle Eocene was evidenced by $\delta^{18}O$ and $\delta^{13}C$ records in the western North Atlantic (Ocean Drilling Program Site 1052) (Wade et al., 2003). The oceanic heat transport caused by a Paleo-Gulf Stream would have contributed further to oceanic climate conditions in Western Europe and to a warmer and wetter climate during the Middle Eocene.

5.3. Middle to Late Eocene seasonality in the Huadian Basin

Few climate reconstructions deal directly with seasonal climatic variations. The differences in temperature and precipitation between summer and winter are as represented by the difference between CMT and WMT and the difference between LMP and HMP, respectively (Wing and Greenwood, 1993; Eldrett and Harding, 2009). These four climatic parameters are critical for determining the mean annual range of temperature (MART) and the mean annual range of precipitation (MARP), allowing us to assess seasonality and continentality (Quan et al., 2012).

Eocene seasonality has not yet been systematically studied in the

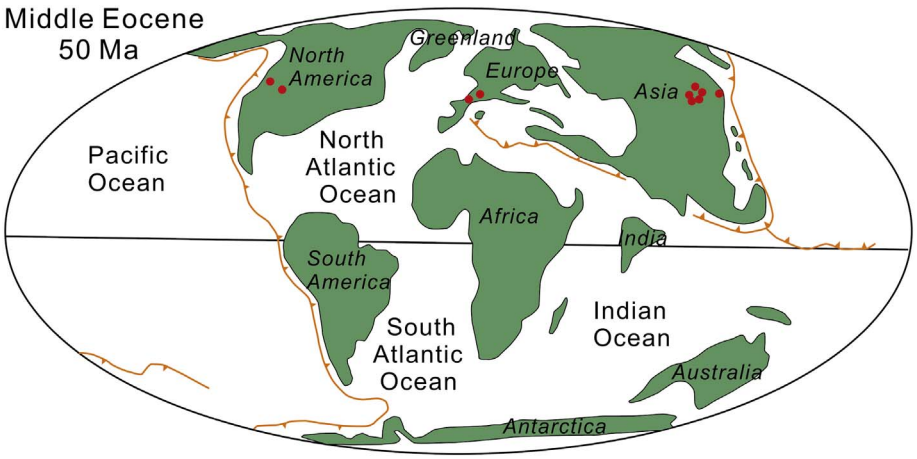

Fig. 10. Palaeographical map of the world (after Scotese, 2001) showing the positions of Huadian, Fushun, Jishu, Hunchun and Dalianhe (Northeast China), Artemo-Tavrichanskii Basin of Southern Primory'e (Russia), Southwest Wyoming and Oregon (North America), Weisselster and Lausitz Basins and Messel (Europe) in middle Eocene.

Huadian Basin. Temperature and precipitation parameters estimated for the Huadian Basin indicate that the mid-late Eocene climate was warm and humid with MAT higher than 13.6 °C, and MAP above 887 mm, typical values for a subtropical climate (Table 1; Fig. 11A). Eocene biomes in the Huadian Basin include subtropical, temperate forests and shrublands (Fig. 11A), largely reflecting seasonal dynamics. A seasonal climate is also apparent in the full mid-late Eocene dataset, where summer and winter temperatures and precipitation patterns can be differentiated (Table 1; Figs. 11B-C).

The temperature of the warmest month does not show much variability in the mid-late Eocene succession (Table 1). WMT and WMP reflect warm summer conditions with abundant rainfall, especially during the deposition of the oil shale horizons (Fig. 11D). Coldest month temperatures reflect relatively warm winters throughout deposition of the Huadian Formation, with CMTs consistently above 1.7 °C. Like the summer climatic parameters, the relationship between

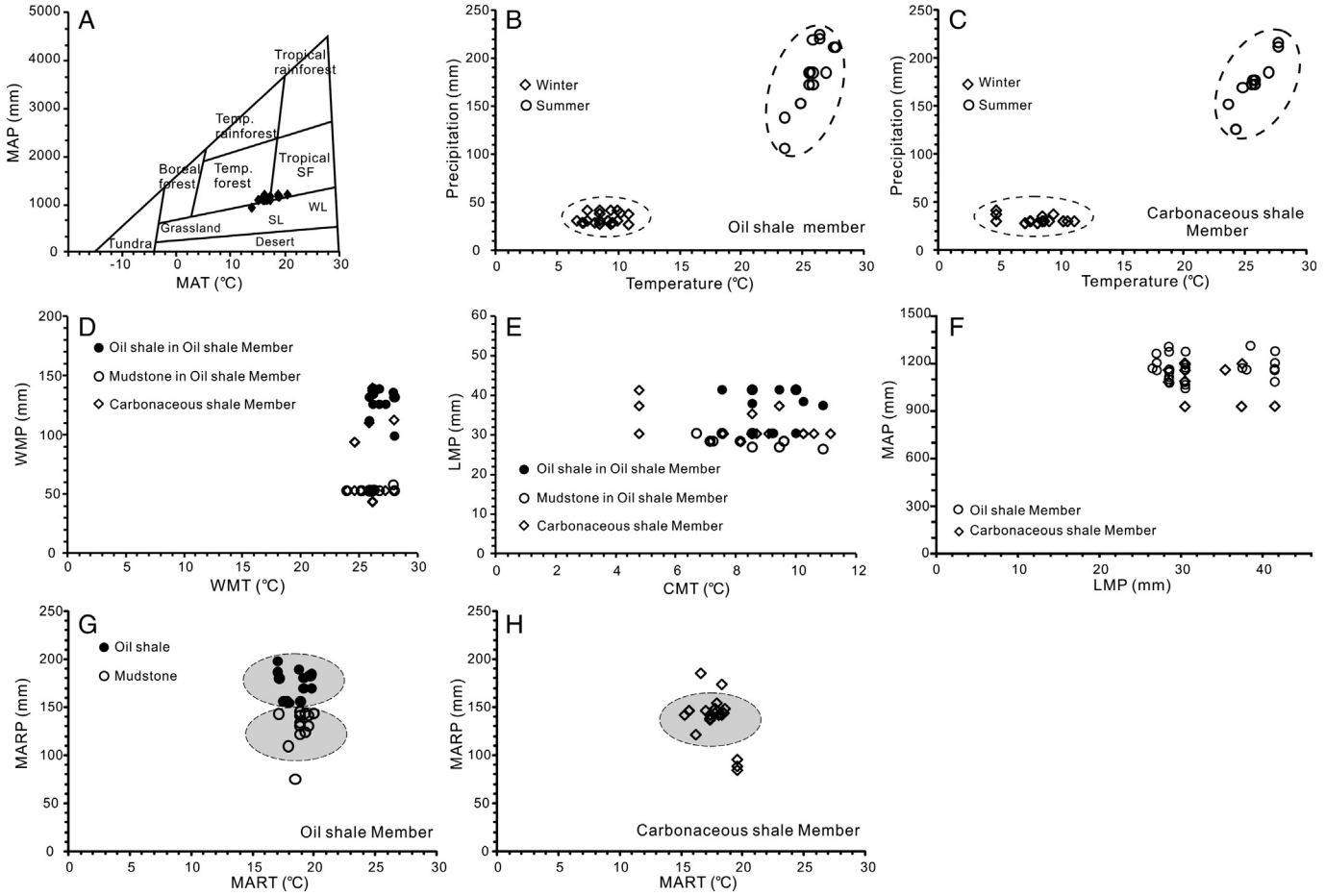

Fig. 11. Mid-late Eocene climatic characteristics illustrated by plotting different combinations of climatic variables. A - Climatic distribution of studied plant assemblages; biomes follow Whittaker (1975); SF, seasonal forest; SL, shrubland; WL, woodland; B - seasonality in all plant assemblages of the oil shale member represented by high annual differentiations in both temperature and precipitation; C - seasonality of the carbonaceous shale member; D - relationship between WMT and WMP, showing the summer climate of the oil shale member is more humid and warmer than that of the carbonaceous shale member; E - Winter climate; F - relationship between LMP and MAP. G - relationship between MART and MARP during the oil shale member, showing two clusters; H - relationship between MART and MARP during the carbonaceous shale member;

winter temperature (CMT) and dry season precipitation (LMP) is different in oil shales compared to other strata (Fig. 11E). Like many basins in northeastern China, e.g., the Fushun, Yilan, and Hunchun basins, most Huadian Basin samples have relatively low LMP values (26.5–41.5 mm), indicating that the mid-late Eocene winter climate was relatively dry. The combination of high MAP and low LMP values estimated from virtually all samples indicate the development of a monsoonal climate (Fig. 11F).

The onset and development of the Asian monsoon system is a topic that has attracted considerable interest. The Asian monsoon is divisible into the South Asian Monsoon (SAM) and the East Asian Monsoon (EAM) (Molnar et al., 2010). Sun and Wang (2005) dated the onset of the East Asian Monsoon to the Late Oligocene-Early Miocene boundary (25–22 Ma). However, the existence of SAM in the Eocene has been postulated (Licht et al., 2014; Shukla et al., 2014), and recent quantitative studies of plant fossils from northeastern China suggest that the EAM may have developed in the early Paleogene and significantly intensified late in the Middle Eocene (Quan et al., 2011, 2012). This study of the Huadian Basin further supports the hypothesis that the East Asian monsoonal climate was already established in northeastern China during the mid-late Eocene.

The drivers of the East Asian Monsoon are complex, and it is likely that the system was strongly affected by the Tibetan-Himalaya mountain uplift (Kitoh, 2004) and topography (Boos and Kuang, 2010; Molnar et al., 2010; Spicer et al., 2016). Uplift of the Tibetan-Himalayan Orogen in northwestern China from the Late Cretaceous into the Cenozoic led to a gradual increase in the air pressure differential between the land and sea, with major implications for the climate of China. The Tibetan Plateau prevents the flow of moist air from the Indian Ocean into inland China, and the climate of China is controlled mainly by the East Asian Monsoon system. The onset of a monsoonal climate in the Huadian Basin may have been related to the development of seasonal alternations in air pressure over Siberia, and the Pacific trade winds. During winter, the climate was influenced by air masses from the Siberian High, causing cold and dry conditions. These were followed by heavy rain in late spring to early summer, as a low-pressure cell developed over warming Siberia, and the Pacific subtropical anticyclone and associated trade winds became stronger. These flows of moist oceanic air converged over northeastern China causing abundant rainfall (Sun and Wang, 2005; Molnar et al., 2010).

5.4. The influence of climate on oil shale formation

Lacustrine oil shales contain abundant organic matter, dominated by authigenic alginite. Climatic change may be an important factor influencing biological productivity, terrigenous influx, and other processes in continental lakes (Wang et al., 1995). Thus, paleoclimate, in combination with tectonic and sedimentary processes, may have been a factor in oil shale formation (Meng et al., 2012a, b). A warm and humid climate enhances chemical weathering, and abundant precipitation can cause a rapid flux of dissolved nutrients into the lake environment, promoting aquatic plankton productivity (Wang and Liu, 1993; Liu et al., 2001). Additionally, high temperatures and high precipitation promote stable density stratification in lacustrine environments (Meng et al., 2012a, b).

Paleoclimatic reconstructions show that the climate during deposition of the Oil Shale Member was warmer and more humid than during deposition of the Carbonaceous Shale Member, with a higher MAP and MAT (Table 1, Fig. 9). Abundant precipitation and a high rate of subsidence during the deposition of the Oil Shale Member caused significant deepening of the Huadian depositional lake, as well as high lacustrine productivity (Meng et al., 2012a, b; Sun et al., 2013), providing abundant organic matter for oil shale formation. This inference is supported by biomarker data, which show that the organic matter preserved in oil shales mostly consists of alginite (lamalginite and telalginite), with only small amounts of terrigenous organic matter (Strobl et al., 2015). This agrees well with the pollen data, which show high concentrations of algae (*Pediastrum* and *Concentricystes*) and aquatic plants (*Potamogeton* and *Lemna*) (Fig. 5T-W).

When comparing the climatic parameters obtained from the different lithologies of the Oil Shale Member and the Carbonaceous Shale Member, significant differences become apparent. The lithofacies within the Oil Shale Member group into two clusters, with oil shales showing high WMT and WMP values, while mudstones yield high WMT but moderate WMP values (Fig. 11D). Oil shales show moderate MART and high MARP, while mudstones have moderate values for both MART and MARP (Fig. 11G). Oil shales also yield higher LMP and CMT values than the mudstones (Fig. 11E). These results indicate that deposition of oil shales took place under conditions characterized by wetter summers and winters than the deposition of mudstones. Oxygen-depleted conditions in deepwater environments, caused by abundant rainfall, favored the preservation of lacustrine organic matter. This stimulated the accumulation of oil shale layers in the deep lake. This relationship suggests that precipitation may be a critical climatic factor driving oil shale formation.

The Carbonaceous Shale Member was deposited in a shallow lake during the final stage of basin evolution, when decreasing tectonic subsidence and increasing sediment supply caused the basin to fill completely (Sun et al., 2013; Meng et al., 2016). Though the climate remained relatively warm and humid during this interval, mean annual temperature and precipitation decreased, as did WMT, CMT, HMP, and LMP. Because precipitation remained high, the rapid input of terrigenous organic matter continued (Strobl et al., 2015). Although WMP, LMP, and WARP values are slightly higher than in the mudstones of the Oil shale Member (Figs. 11D, E and H), this interval does not contain oil shales, though carbonaceous shales and coals are developed locally; the low TOC content of the Carbonaceous Shale Member primarily reflects the poor preservation of organic matter in a shallow lake environment.

6. Conclusions

Middle to Late Eocene climatic change in the Huadian Basin of northeastern China can be reconstructed quantitatively based on palynological records. A total of eighty-five palynomorph genera and one hundred palynomorph species were identified. The nearest living relatives of the recovered palynotaxa suggest that subtropical evergreen and deciduous broad-leaved forests were present during the deposition of the Huadian Formation. Based on the CA method, paleoclimatic results demonstrate that a warm, humid subtropical climate predominated in the Huadian Basin during the mid-late Eocene, with MAT above 13.6 °C and MAP over 887 mm. Middle to Late Eocene seasonality is reflected in the evident differences in both temperature and precipitation between summer and winter. This evidence supports the hypothesis that the East Asian Monsoon was already prevalent in northeastern China at that time. This mid-late Eocene monsoon was probably driven by the development of an alternating high- and low-pressure system depending on the seasonal climate of Siberia, in combination with Pacific trade winds. Consistent trends in various climatic parameters recorded in the Huadian Basin clearly reflect a moderate but detectable decrease in temperature and precipitation during the transition from the Oil Shale Member to the Carbonaceous Shale Member. Those and other paleoclimatic data from other mid-late Eocene basins in northeastern China were compared with North American and European climate reconstructions. Similar trends in temperature and precipitation across different continents strongly support the existence of a globally cooler phase in the Middle Eocene.

Climatic changes, especially changes in precipitation, seem to play an important role in controlling oil shale formation. A warmer and more humid climate, with abundant precipitation and high subsidence rates, predominated during deposition of the Oil Shale Member, causing an increase in lake productivity. Abundant organic matter and oxygen-depleted conditions favored the preservation of lacustrine organic

matter and the accumulation of abundant oil shale horizons especially during the periods of highest precipitation during the summer monsoon. As the climate gradually became cooler and less humid during deposition of the Carbonaceous Shale Member, the environment transitioned to an ephemeral, shallow lake, under the influence of decreasing tectonic activity and increasing sediment supply. A rapid flux of terrigenous organic matter, and poor conditions for organic preservation, resulted in the development of carbonaceous shale and, locally, coal.

Acknowledgments

We would like to thank Wang Lijun (Engineer at the First Geological Survey of Jilin Province) for his help with core measurements, and Zhang Shuqin (Jilin University) for her advice on palynological identification and interpretation. We are also grateful to the chief editor Thomas Algeo, guest editor Zhongshi Zhang and the reviewer Torsten Utescher for their suggestions and comments, which significantly improved the quality of the manuscript. This study was financially supported by the National Science Foundation of China (Grant No. 41302075), the Doctoral Foundation of China (Grant No. 20110061120066), the China Postdoctoral Science Foundation (Grant No. 2013M541291), and Science and Technology Development Project of Jilin Province, China (Grant No. 20150622003JC). This paper is a contribution to NECLIME (Neogene climate evolution in Eurasia).

Appendix A. Supplementary data

Supplementary data to this article can be found online at https://doi.org/10.1016/j.palaeo.2017.11.036.

References

Abelson, M., Agnon, A., Almogi-Labin, A., 2008. Indications for control of the Iceland plume on the Eocene–Oligocene “greenhouse–icehouse” climate transition. Earth Planet. Sci. Lett. 265 (1), 33–48.
Bai, Y.Y., Liu, Z.J., Sun, P.C., Liu, R., Hu, X.F., Zhao, H.Q., Xu, Y.B., 2015. Rare earth and major element geochemistry of Eocene fine-grained sediments in oil shale-and coal-bearing layers of the Meihe Basin, Northeastern China. J. Asian Earth Sci. 97, 89–101.
Bijl, P.K., Schouten, S., Sluijs, A., Reichart, G.-J., Zachos, J.C., Brinkhuis, H., 2009. Early Palaeogenetemperature evolution of the southwest Pacific Ocean. Nature 461, 776–779.
Boos, W.R., Kuang, Z., 2010. Dominant control of the South Asian monsoon by orographic insulation versus plateau heating. Nature 463, 218–222.
Bruch, A.A., Mosbrugger, V., 2002. Palaeoclimate versus vegetation reconstruction-palynological investigation on Oligocene sequence of the Sava Basin, Slovenia. Rev. Palaeobot. Palynol. 122, 117–141.
Bruch, A.A., Utescher, T., Mosbrugger, V., 2011. Precipitation patterns in the Miocene of Central Europe and the development of continentality. Palaeogeogr. Palaeoclimatol. Palaeoecol. 204, 202–211.
Bureau of Geology and Mineral Resources of Jilin Province, 1988. Regional Geology of Jilin Province. Geological Publishing House, Beijing, pp. 1–698 (in Chinese).
Dall'Antonia, B., Bossio, A., Guernet, C., 2003. The Eocene/Oligocene boundary and the psychrospheric event in the Tethys as recorded by deep-sea ostracods from the Massignano Global Boundary Stratotype Section and Point, Central Italy. Mar. Micropaleontol. 48 (1), 91–106.
Eldrett, J.S., Harding, I.C., 2009. Palynological analysis of Eocene to Oligocene sediments from DSDP Site 338, Outer Voring Plateau. Mar. Micropaleontol. 73, 226–240.
Feurdean, A., Klotz, S., Brewer, S., Mosbrugger, V., Tamas, T., Wohlfarth, B., 2008. Lateglacial climate development in NW Romania-comparative results from three quantitative pollen-based methods. Palaeogeogr. Palaeoclimatol. Palaeoecol. 265, 121–133.
Greenwood, D.R., Wing, S.L., 1995. Eocene continental climates and latitudinal temperature gradients. Geology 23, 1044–1048.
Greenwood, D.R., Basinger, J.F., Smith, R.Y., 2010. How wet was the Arctic Eocene rain forest? Estimates of precipitation from Paleogene Arctic macrofloras. Geology 38, 15–18.
Grein, M., Utescher, T., Wilde, V., Roth-Nebelsick, A., 2011. Reconstruction of the middle Eocene climate of Messel using palaeobotanical data. N. Jb. Geol. Paläont. (Abh.) 260 (3), 305–318.
Grimm, E.C., 2011. TILIA Software Version 1.7.16. Illinois State Museum, Research and Collection Center, Springfield USA.
Hao, H., Ferguson, D.K., Feng, G.P., Ablaev, A., Wang, Y.F., Li, C.S., 2010. Early Paleocene vegetation and climate in Jiayin, NE China. Clim. Chang. 99, 547–566.
He, C.X., Tao, J.R., 1997. A study on the Eocene flora in Yilan County, Heilongjiang. Acta Phys. Sin. 35, 249–256 (in Chinese with English abstract).
Hollis, C.J., Handley, L., Crouch, E.M., Morgans, H.E.G., Baker, J.A., Creech, J., Collins, K.S., Gibbs, S.J., Huber, M., Schouten, S., Zachos, J.C., Pancost, R.D., 2009. Tropical sea temperatures in the high-latitude South Pacific during the Eocene. Geology 37, 99–102.
Hong, Y.C., Yang, Z.Q., Wang, S.T., Sun, X.J., Du, N.Q., Sun, M.R., Li, Y.G., 1980. A Research on the Strata and Palaeontology of the Fushun Coal Field in Liaoning Province. Science Press, Beijing (in Chinese).
Houben, A.J., van Mourik, C.A., Montanari, A., Coccioni, R., Brinkhuis, H., 2012. The Eocene-Oligocene transition: changes in sea level, temperature or both? Palaeogeogr. Palaeoclimatol. Palaeoecol. 335, 75–83.
Huang, Q.H., Huang, F.T., Zhang, Y., Chen, C.R., Kong, H., Jin, X.X., 1998. New advance in the tertiary strata study of the Tangyuan rift. J. Stratigr. 22 (1), 73–80 (in Chinese with English abstract).
Irving, E., 2008. Why earth became so hot 50 million years ago and why it then cooled. Proc. Natl. Acad. Sci. 105 (42), 16061–16062.
Ivanov, D., Ashraf, A.R., Mosbrugger, V., Palamarev, E., 2002. Palynological evidence for Miocene climate change in Forecarpathian Basin (Central Paratethys, NW Bulgaria). Palaeogeogr. Palaeoclimatol. Palaeoecol. 178, 19–37.
Ivanov, D.A., Ashraf, A.R., Mosbrugger, V., 2007. Late Oligocene and Miocene climate and vegetation in the Eastern Paratethys area (northeast Bulgaria), based on pollen data. Palaeogeogr. Palaeoclimatol. Palaeoecol. 255 (3), 342–360.
Ivany, L.C., Patterson, W.P., Lohmann, K.C., 2000. Cooler winters as a possible cause of mass extinctions at the Eocene/Oligocene boundary. Nature 407, 887–890.
Kelts, K., Hsü, K.J., 1978. Freshwater carbonate sedimentation. In: Lerman, A. (Ed.), Lakes: Chemistry, Geology, Physics. Spring-Verlag, Berlin, pp. 290–350.
Kitoh, A., 2004. Effects of mountain uplift on East Asian summer climate investigated by a coupled atmosphere–ocean GCM. Am. Meteorol. Soc. 17, 783–802.
Kou, X.Y., 2005. Studies on Quantitative Reconstruction of Cenozoic Climates in China by Palynological Data. Doctoral dissertation. Graduate School of Chinese Academy of Sciences, Beijing (in Chinese with English abstract).
Kou, X.Y., Ferguson, D.K., Xu, J.X., Wang, Y.F., Li, C.S., 2006. The reconstruction of paleovegetation and paleoclimate in the Late Pliocene of west Yunnan, China. Clim. Chang. 77 (324), 431–448.
Krapp, M., Jungclaus, J.H., 2011. The Middle Miocene climate as modeled in an atmosphere-ocean-biosphere model. Clim. Past Discuss. 7, 1935–1972.
Liang, M.M., Wang, Y.F., Li, C.S., 2001. Palaeovegetation succession and quantitative palaeoclimate reconstruction of the Miocene Shanwang assemblage. J. Palaeogeogr. 3 (3), 11–20 (in Chinese with English abstract).
Liang, M.M., Bruch, A.A., Collinson, M., Mosbrugger, V., Li, C.S., Sun, Q.G., Hilton, J., 2003. Testing the climatic estimates from different palaeobotanical methods: an example from the Middle Miocene Shanwang flora of China. Palaeogeogr. Palaeoclimatol. Palaeoecol. 198, 279–301.
Licht, A., Van Cappelle, M., Abels, H.A., Ladant, J.B., Trabucho-Alexandre, J., France-Lanord, C., Donnadieu, Y., Vandenberghe, J., Rigaudier, T., Lecuyer, C., Terry Jr., D., Adriaens, R., Boura, A., Guo, Z., Soe, Aung Naing, Quade, J., Dupont-Nivet, G., Jaeger, J.J., 2014. Asian monsoons in a late Eocene greenhouse world. Nature 513, 501–506.
Liu, J., Chang, M.M., 2009. A new Eocene catostomid (Teleostei: Cypriniformes) from northeastern China and early divergence of Catostomidae. Sci. China Ser. D Earth Sci. 52 (2), 189–202.
Liu, C.L., Zhao, Q.H., Wang, P.X., 2001. Correlation between carbon and oxygen isotopic ratios of laxustrine carbonates and types of oil producing paleolakes. Chem. Aust. 30 (4), 363–367.
Liu, Z.J., Meng, Q.T., Liu, R., Dong, Q.S., 2009. Geochemical characteristics of oil shale of Eocene Jijuntun Formation and its geological significance, Fushun Basin. Acta Petrol. Sin. 25 (10), 2340–2350 (in Chinese with English abstract).
Liu, R., Liu, Z.J., Liu, S.Y., Liu, D.Q., Li, B.Y., Yang, X.H., Xu, Y.B., 2012. Coal and oil shale occurrence characteristic and metallogenic regularity in Yilan Basin. J. China Coal Soc. 37 (5), 776–781 (in Chinese with English abstract).
Manchester, S.R., 2000. Late Eocene fossil plants of the John Day Formation, Wheeler County, Oregon. Or. Geol. 62 (3), 51–63.
Manchester, S.R., Chen, Z., Geng, B., Tao, J., 2005. Middle Eocene flora of Huadian, Jilin Province, Northeast China. Acta Palaeobotanica 45 (1), 3–26.
Meng, Q.T., 2010. Research on Petrologic and Geochemical Characteristics of Eocene Oil Shale and its Enrichment Regularity, Huadian Basin. Doctoral dissertation. Jilin University, Changchun (in Chinese with English abstract).
Meng, Q.T., Liu, Z.J., Bruch, A.A., Liu, R., Hu, F., 2012a. Palaeoclimatic evolution during Eocene and its influence on oil shale mineralization, Fushun Basin, China. J. Asian Earth Sci. 45, 95–105.
Meng, Q.T., Liu, Z.J., Hu, F., Sun, P.C., Zhou, R.J., Zhen, Z., 2012b. Productivity of Eocene ancient lake and enrichment mechanism of organic matter in Huadian Basin. Journal of China University of Petroleum 36 (5), 38–44 (in Chinese with English abstract).
Meng, Q.T., Liu, Z.J., Hu, F., Sun, P.C., Liu, R., Zhou, R.J., Zhen, Z., 2013. Geochemical characteristics of Eocene oil shale and its geological significances in Huadian Basin. J. Jilin Univ. (Earth Sci. Ed.) 43 (2), 390–399 (in Chinese with English abstract).
Meng, Q.T., Liu, Z.J., Sun, P.C., Jia, J.L., Hu, F., 2016. Sequence stratigraphy and sedimentary environment of the Eocene Huadian formation in the Huadian Basin (NE China): implications for oil shale distribution. Russian Journal of Pacific Geology (Russian Edition) 35 (6), 81–101.
Molnar, P., Boos, W.R., Battisti, D.S., 2010. Orographic controls on climate and paleoclimate of Asia: thermal and mechanical roles for the Tibetan Plateau. Annu. Rev. Earth Planet. Sci. 38, 77–102.
Mosbrugger, V., Utescher, T., 1997. The coexistence approach-a method for quantitative reconstructions of tertiary terrestrial palaeoclimate data using plant fossils. Palaeogeogr. Palaeoclimatol. Palaeoecol. 134, 61–86.

Mosbrugger, V., Utescher, T., Dilcher, D.L., 2005. Cenozoic continental climatic evolution. PNAS 102, 14964–14969.
Passchier, S., Pearce, R.B., Kearns, L.E., 2009. Evidence for middle Eocene Arctic sea ice from diatoms and ice-rafted debris. Nature 460, 376–379.
Persico, D., Villa, G., 2004. Eocene-Oligocene calcareous nannofossils from Maud Rise and Kerguelen Plateau (Antarctica): paleoecological and paleoceanographic implications. Mar. Micropaleontol. 52 (1), 153–179.
Prothero, D.R., Berggren, W.A., 1992. Eocene-Oligocene Climatic and Biotic Evolution. Princeton University Press, Oxford, United Kingdom.
Quan, C., Liu, Y.S., Utescher, T., 2011. Paleogene evolution of precipitation in northeast China supporting the middle Eocene intensification of the East Asian monsoon. PALAIOS 26, 743–753.
Quan, C., Liu, Y.S., Utescher, T., 2012. Paleogene temperature gradient, seasonal variation and climate evolution of northeast China. Palaeogeogr. Palaeoclimatol. Palaeoecol. 313–314, 150–163.
Roth-Nebelsick, A., Utescher, T., Mosbrugger, V., Diester-Haass, L., Walther, H., 2004. Changes in atmospheric CO_2 concentrations and climate from the Late Eocene to Early Miocene: palaeobotanical reconstruction based on fossil floras from Saxony, Germany. Palaeogeogr. Palaeoclimatol. Palaeoecol. 205, 43–67.
Scotese, C.R., 2001. Plate Tectonic Map and Continental Drift Animations. PALEOMAP Project. http://www.scotese.com.
Shi, J.Z., Liu, Z.J., Liu, R., Du, J.F., Zhang, J., Liu, F., 2008. Quantitative reconstruction of the Eocene palaeoclimate in the Fushun Basin, Liaoning Province. J. Jilin Univ. (Earth Sci. Ed.) 38, 50–55 (in Chinese with English abstract).
Shukla, A., Mehrotra, R.C., Spicer, R.A., Spicer, T.E.V., Kumar, M., 2014. Cool equatorial terrestrial temperatures and the South Asian monsoon in the Early Eocene: evidence from the Gurha Mine, Rajasthan, India. Palaeogeogr. Palaeoclimatol. Palaeoecol. 412, 187–198.
Smith, K.T., Schaal, S.F.K., Sun, W., Li, C.T., 2011. Acrodont Iguanians (Squamata) from the Middle Eocene of the Huadian Basin of Jilin Province, China, with a critique of the taxon “Tinosaurus”. Vertebrata Palasiatica 49 (1), 69–84.
Spicer, R.A., Yang, J., Herman, A.B., Kodrul, T., Maslova, N., Spicer, T.E.V., Aleksandrova, G., Jin, J.H., 2016. Asian Eocene monsoons as revealed by leaf architectural signatures. Earth Planet. Sci. Lett. 449, 61–68.
Strobl, S.A.I., Sachsenhofer, R.F., Bechtel, A., Meng, Q.T., Sun, P.C., 2015. Deposition of coal and oil shale in NE China: the Eocene Huadian Basin compared to the coeval Fushun Basin. Mar. Pet. Geol. 64, 347–362.
Su, T., Xing, Y.W., Yang, Q.S., Zhou, Z.K., 2009. Reconstruction of mean annual temperature in Chinese Eocene paleofloras based on leaf margin analysis. Acta Palaeontol. Sin. 48 (1), 65–72 (in Chinese with English abstract).
Sun, X., Wang, P., 2005. How old is the Asian monsoon system?—Palaeobotanical records from China. Palaeogeogr. Palaeoclimatol. Palaeoecol. 222 (3), 181–222.
Sun, P.C., Sachsenhofer, R.F., Liu, Z.J., Strobl, S.A.I., Meng, Q.T., Liu, R., Zhen, Z., 2013. Organic matter accumulation in the oil shale-and coal-bearing Huadian Basin (Eocene; NE China). Int. J. Coal Geol. 105, 1–15.
Tripati, A., Backman, J., Elderfield, H., Ferretti, P., 2005. Eocene bipolar glaciation associated with global carbon cycle changes. Nature 436, 341–346.
Uhl, D., Mosbrugger, V., Bruch, A.A., Utescher, T., 2003. Reconstructing palaeotemperatures using leaf floras-case studies for a comparison of leaf margin analysis and the coexistence approach. Rev. Palaeobot. Palynol. 126, 49–64.
Utescher, T., Mosbrugger, V., 2007. Eocene vegetation patterns reconstructed from plant diversity-a global perspective. Palaeogeogr. Palaeoclimatol. Palaeoecol. 247, 243–271.
Utescher, T., Mosbrugger, V., Ivanov, D., Dilcher, D.L., 2011a. Present-day climatic equivalents of European Cenozoic climates. Earth Planet. Sci. Lett. 284, 544–552.
Utescher, T., Bruch, A.A., Micheels, A., Mosbrugger, V., Popova, S., 2011b. Cenozoic climate gradients in Eurasia—a palaeo-perspective on future climate change? Palaeogeogr. Palaeoclimatol. Palaeoecol. 304 (3), 351–358.
Utescher, T., Bruch, A.A., Erdei, B., François, L., Ivanov, D., Jacques, F.M.B., Kern, A.K., Liu, Y.S., Mosbrugger, V., Spicer, R.A., 2014. The Coexistence Approach—theoretical background and practical considerations of using plant fossils for climate quantification. Palaeogeogr. Palaeoclimatol. Palaeoecol. 410, 58–73.
Utescher, T., Bondarenko, O.V., Mosbrugger, V., 2015. The Cenozoic Cooling–continental signals from the Atlantic and Pacific side of Eurasia. Earth Planet. Sci. Lett. 415, 121–133.
Via, R.K., Thomas, D.J., 2006. Evolution of Atlantic thermohaline circulation: Early Oligocene onset of deep-water production in the North Atlantic. Geology 34, 441–444.
Villa, G., Fioroni, C., Pea, L., Bohaty, S., Persico, D., 2008. Middle Eocene-late Oligocene climate variability: calcareous nannofossil response at Kerguelen Plateau, Site 748. Mar. Micropaleontol. 69, 173–192.
Wade, B.S., Kroon, D., Pälike, H., 2003. Fluctuations in the position of the Proto Gulf Stream: evidence from high-resolution stable isotope results. In: XXIII General Assembly of the International Union of Geophysics and Geodesy. IUGG 2003: The State of the Planet. Sapporo, Japan, 30 June–11, July 2003. Dent. Abstr..
Wang, Z.G., 1998. Reconstruction of past 5000 year humidity changes of Northeast China using $\delta^{13}C$ values of peat cellulose in Jinchuan Region, Jilin Province. Bull. Mineral. Petrol. Geochem. 17 (1), 52–54 (in Chinese with English abstract).
Wang, B.Y., Li, C.T., 1990. First Paleogene mammalian fauna from Northeast China. Vertebrata Palasiatica 28 (3), 165–205 (in Chinese with English abstract).
Wang, P.X., Liu, C.L., 1993. Research Method of Palaeolimnology in Oil-Bearing Basin. Ocean Press, Beijing (in Chinese).
Wang, H.Z., Mei, H.M., 1998. Paleolimnological information from the oil shale in the lower part of Sha 3 Formation in Dongying Depression. Journal of Tongji University 26 (3), 315–319 (in Chinese with English abstract).
Wang, D.P., Liu, L., Zhang, L.P., Lv, C.J., 1995. The Palaeoclimate, Depositional Cycle and Sequence Stratigraphy of Songliao Basin. Press of Jilin University, pp. 25–67 (in Chinese with English abstract).
Wang, Y.F., Yang, J., Xu, J.X., Zhao, L.C., Jiang, H.E., Cheng, Y.M., Yi, T.M., Wang, Q., Ma, Q.W., Yao, Y.F., 2009. Research highlights on the evolution of Cenozoic plants and the reconstruction of palaeoclimate and palaeoenvironments in China. Acta Palaeontol. Sin. 48 (3), 569–576 (in Chinese with English abstract).
Wang, Q., Ferguson, D.K., Feng, G.P., Ablaev, A.G., Wang, Y.F., Yang, J., Li, Y.L., Li, C.S., 2010. Climatic change during the Palaeocene to Eocene based on fossil plants from Fushun, China. Palaeogeogr. Palaeoclimatol. Palaeoecol. 295, 323–331.
Wei, C.Y., Wan, G.J., 1995. Research on the past climate changes from lacustrine deposit. Geological Geochemistry 23 (1), 54–57 (in Chinese).
Whittaker, R.H., 1975. Communities and ecosystems. MacMillan, New York.
Wilf, P., 2000. Late Paleocene-early Eocene climate changes in southwestern Wyoming: paleobotanical analysis. Geol. Soc. Am. Bull. 112, 292–307.
Wilf, P., Wing, S.L., Greenwood, D.R., Greenwood, C.L., 1998. Using fossil leaves as paleoprecipitation indicators: an Eocene example. Geology 26, 203–206.
Wing, S.L., Greenwood, D.R., 1993. Fossils and fossil climates: the case for equable continental interiors in the Eocene. Philos. Trans. R. Soc., B 341, 243–252.
Wing, S.L., Bao, H.M., Koch, P.L., 1999. An early Eocene cool period? Evidence for continental cooling during the warmest part of the Cenozoic. In: Huber, B.T., Macleod, K., Wing, S.L. (Eds.), Warm Climates in Earth History. Cambridge University Press, Cambridge, pp. 197–237.
Wolfe, J.A., 1993. A method of obtaining climatic parameters from leaf assemblages. U.S. Geol. Surv. Bull. 2041, 1–71.
Xia, K., Su, T., Liu, Y.S., Xing, Y.W., Jacques, F.M.B., Zhou, Z.K., 2009. Quantitative climate reconstruction of the late Miocene Xialongtan megaflora from Yunnan, southwest China. Palaeogeogr. Palaeoclimatol. Palaeoecol. 276 (1), 80–86.
Xu, J.X., Ferguson, D.K., Li, C.S., Wang, Y.F., 2008. Late Miocene vegetation and climate of the Lühe region in Yunnan, southwestern China. Rev. Palaeobot. Palynol. 148, 36–59.
Xu, S.C., Liu, Z.J., Dong, Q.S., Liu, S.Y., Liu, R., Meng, Q.T., 2012. Eocene sedimentary evolution and its control over coal & oil shale development in Fushun Coalfield. Journal of China University of Petroleum (Edition of Natural Science) 2, 007.
Yang, J., Wang, Y.F., Sun, Q.G., Li, C.S., 2002. Quantitative studies on paleoelevation and paleoclimate of Shanwang Miocene basin, east China. Earth Science Frontiers (China University of Geosciences Beijing) 9 (3), 183–188 (in Chinese with English abstract).
Yang, J.G., Huang, Q.H., Wu, C.D., Wu, H.Y., 2004. Sequences and ages of the Paleogene and Neogene strata in the Tangyuan Rift, Heilongjiang. J. Stratigr. 28 (2), 168–172 (in Chinese with English abstract).
Yao, Y.F., Subir, B., Ferguson, D.K., Mosbrugger, V., Paudayal, K.N., Jin, J.H., Li, C.S., 2009. Reconstruction of paleovegetation and paleoclimate in the Early and Middle Eocene, Hainan Island, China. Clim. Chang. 92 (122), 169–189.
Zachos, J.C., Stott, L.D., Lohmann, K.C., 1994. Evolution of early Cenozoic marine temperatures. Paleoceanography 9, 353–387.
Zachos, J.C., Pagani, M., Sloan, L., Thomas, E., Billups, K., 2001. Trends, rhythms and aberrations in global climate 65 Ma to present. Science 292, 686–696.
Zachos, J.C., Dickens, G.R., Zeebe, R.E., 2008. An early Cenozoic perspective on greenhouse warming and carbon-cycle dynamics. Nature 451, 279–293.
Zhang, F., Wang, K.W., Liu, L., 2007. Stratigraphic sequence of Neogence system in Yishu Graben. J. Jilin Univ. (Earth Sci. Ed.) 37 (1), 112–119 (in Chinese with English abstract).
Zhao, L.C., Wang, Y.F., Liu, C.J., 2004. Climatic implications of fruits and seed assemblage from Miocene of Yunnan, southwestern China. Quat. Int. 117, 81–89.
Zhou, J.J., Sun, J.R., 1985. The Late of Early Eocene fishes were found in Huadian Basin, Jilin Province in China. Vertebrata Palasiatica 23 (2), 170 (in Chinese).
Zhu, G.Y., Jin, Q., Zhang, S.C., Dai, J.X., Wang, G.M., Zhang, L.Y., Li, J., 2005. Characteristics and origin of deep lake oil shale of the Shahejie Formation of Paleogene in Dongying Sag, Jiyang Depression. J. Palaeogeogr. 7 (1), 59–69 (in Chinese with English abstract).